STUDIES OF HOMOGENEOUS AND HETEROGENEOUS HYDRAZINE DECOMPOSITION FOR MONOPROPELLANT PROPULSION SYSTEMS

S. W. Benson, et al

Stanford Research Institute

Prepared for:

Air Force Office of Scientific Research

25 July 1975

Annual Report

Covering the Period June 1 1974 through May 31, 1975

STUDIES OF HOMOGENEOUS AND HETEROGENEOUS HYDRAZINE DECOMPOSITION FOR MONOPROPELLANT PROPULSION SYSTEMS

By S W BENSON, J L FALCONER, D M GOLDEN, S E STEIN, H WISE, and B J WOOD

Prepared for

AIR FORCE OFFICE OF SCIENTIFIC RESEARCH
1400 WILSON BOULEVARD
ARLINGTON, VIRGINIA 22209
Attention CAPTAIN L R LAWRENCE

AFOSR CONTRACT F44620 73 C 0069

STANFORD RESEARCH INSTITUTE
Menlo Park, California 94025 · U.S.A

SECURITY CLASSIFICATION OF THIS PAGE (When Data Entered)

REPORT DOCUMENTATION PAGE

READ INSTRUCTIONS BEFORE COMPLETING FORM

1. REPORT NUMBER: AFOSR - TR - 75 - 1203	2. GOVT ACCESSION NO.
3. RECIPIENT'S CATALOG NUMBER: AD-A015 902	
4. TITLE (and Subtitle): STUDIES OF HOMOGENEOUS AND HETEROGENEOUS HYDRAZINE DECOMPOSITION FOR MONOPROPELLANT PROPULSION SYSTEMS	5. TYPE OF REPORT & PERIOD COVERED: INTERIM, 1 June 1974 - 31 May 1975
	6. PERFORMING ORG. REPORT NUMBER
7. AUTHOR(s): S W BENSON, S E STEIN, J L FALCONER, H WISE, D M GOLDEN, B J WOOD	8. CONTRACT OR GRANT NUMBER(s): F44620-73-C-0069
9. PERFORMING ORGANIZATION NAME AND ADDRESS: STANFORD RESEARCH INSTITUTE, MENLO PARK, CALIFORNIA 94025	10. PROGRAM ELEMENT, PROJECT, TASK AREA & WORK UNIT NUMBERS: 681308, 9711-01, 61102F
11. CONTROLLING OFFICE NAME AND ADDRESS: AIR FORCE OFFICE OF SCIENTIFIC RESEARCH/NA, 1400 WILSON BOULEVARD, ARLINGTON, VIRGINIA 22209	12. REPORT DATE: July 1975
	13. NUMBER OF PAGES: 72
14. MONITORING AGENCY NAME & ADDRESS (if different from Controlling Office)	15. SECURITY CLASS. (of this report): UNCLASSIFIED
	15a. DECLASSIFICATION DOWNGRADING SCHEDULE

16. DISTRIBUTION STATEMENT (of this Report)

Approved for public release; distribution unlimited.

17. DISTRIBUTION STATEMENT (of the abstract entered in Block 20, if different from Report)

18. SUPPLEMENTARY NOTES

19. KEY WORDS (Continue on reverse side if necessary and identify by block number)

HYDRAZINE
MONOPROPELLANTS
SPACE PROPULSION

20. ABSTRACT (Continue on reverse side if necessary and identify by block number)

Surface studies on Shell-405 catalyst by temperature-programmed desorption, surface-area titration, and Auger electron spectroscopy point to a loss in active surface area of iridium caused by crystallite sintering and accumulation of surface impurities following exposure to hydrazine. The heterogeneous decomposition kinetics point to a reaction order of ½ on silica surfaces and of unity on Shell-405 catalyst. The products of decomposition are temperature dependent. These results provide some insight into the causes of catalyst deactivation resulting from surface changes of the active metal component of Shell-405 catalyst, i.e.,

DD FORM 1 JAN 73 1473 EDITION OF 1 NOV 65 IS OBSOLETE

UNCLASSIFIED

the iridium crystallites. It is expected that such catalyst changes will exert a profound influence on the ignition characteristics of the monopropellant rocket thruster.

STANFORD RESEARCH INSTITUTE
Menlo Park, California 94025, U.S.A.

Annual Report *July 25, 1975*

Covering the Period June 1, 1974 through May 31, 1975

STUDIES OF HOMOGENEOUS AND HETEROGENEOUS HYDRAZINE DECOMPOSITION FOR MONOPROPELLANT PROPULSION SYSTEMS

By S. W. BENSON, J. L. FALCONER, D. M. GOLDEN, S. E. STEIN, H. WISE, and B. J. WOOD

Prepared for

AIR FORCE OFFICE OF SCIENTIFIC RESEARCH
1400 WILSON BOULEVARD
ARLINGTON, VIRGINIA 22209
Attention CAPTAIN L. R. LAWRENCE

AFOSR CONTRACT F44620-73-C-0069

SRI Project PYU-2716

Approved by:

MARION E. HILL, *Director*
Chemistry Laboratory

CHARLES J. COOK, *Executive Director*
Physical Sciences Division

CONTENTS

I OBJECTIVE

The overall objective of this study is the elucidation of the gradual activity decay exhibited by hydrazine fuel thrusters operating in a pulse mode and using granular-supported iridium catalysts (Shell-405). During the current program year the experimental effort comprised two concurrent parts: (1) a study of the surface properties of Shell-405 catalyst (alumina-supported iridium) on exposure to hydrazine, and (2) studies of heterogeneous hydrazine decomposition on silica and Shell-405 catalyst. In this report we describe the work completed during the contract period.

II SUMMARY

Surface studies on Shell-405 catalyst by temperature-programmed desorption, surface-area titration, and Auger electron spectroscopy point to a loss in active surface area of iridium caused by crystallite sintering and accumulation of surface impurities following exposure to hydrazine. The heterogeneous decomposition kinetics point to a reaction order of 1/2 on silica surfaces and of unity on Shell-405 catalyst. The products of decomposition are temperature dependent. These results provide some insight into the causes of catalyst deactivation resulting from surface changes of the active metal component of Shell-405 catalyst, i.e., the iridium crystallites. It is expected that such catalyst changes will exert a profound influence on the ignition characteristics of the monopropellant rocket thruster.

III EXPERIMENTS

A. Surface Properties of Shell-405 Catalyst (Ir/Al_2O_3)

The objective of this part of our study was to identify the species retained on the surface of an iridium-on-alumina catalyst (Shell-405) following hydrazine decomposition in order to examine their effect on catalytic activity. The surface species were studied by the technique of temperature programmed desorption (TPD). The same apparatus was also used to study product stoichiometry as a function of catalyst temperature for injections of N_2H_4 aliquots. In addition, the surface of the catalyst was characterized by Auger electron spectroscopy (AES) and a surface area titration technique (SAT). Results are presented for fresh Shell-405 catalyst samples and for samples exposed to hydrazine in rocket thrusters.

1. Temperature Programmed Desorption (TPD)

The TPD technique is particularly suitable for the study of adsorbed species and their binding energies on catalyst surfaces. Also, it offers a means of identifying those adspecies that are retained by the catalyst after exposure to reactants. In these experiments the catalyst was placed in a microreactor apparatus, and a helium stream flowed over it at one atmosphere pressure. Aliquots of liquid hydrazine were injected into the helium stream and, after attainment of steady-state conditions, the catalyst temperature was raised at a prescribed linear rate. The concentration of the desorbing species in the helium stream, which was continuously sampled by a mass spectrometer, was proportional to their desorption rate from the surface. A plot of this desorption rate as a function of catalyst temperature, labeled a desorption spectrum, yielded information about surface coverages and binding states.

TPD studies were completed on the catalyst samples supplied by Rocket Research Corporation (RRC) of Redmond, Washington. Both fresh samples of Shell-405 catalyst and samples that had been exposed to 1097 moles of N_2H_4 per gram of catalyst in a rocket thruster were examined. The results will be briefly summarized here; further details are to be found in the attached Technical Report (Appendix 1).

Following exposure to hydrazine, the catalyst was heated at 2 Ks^{-1}. Molecular nitrogen, hydrogen, ammonia, and water were observed among the desorption products. The desorption spectra were similar to those obtained following ammonia exposure to the same catalyst. Also, the TPD results for Shell-405 exhibited some similarities to the flash desorption results from polycrystalline iridium foil.

The surface coverages of adsorbed species had decreased on the catalyst exposed to 1097 moles N_2H_4. The decrease correlated with the decrease in metal surface area (cf. following section). However, no differences were observed in binding states or relative surface coverages of the various adspecies on the fresh and used catalysts.

The Shell-405 sample supplied by the Rocket Propulsion Laboratory (RPL), Edwards AFB, Edwards, California, exhibited somewhat different surface properties, as summarized in Table 1. It should be noted that the RPL sample was more difficult to reduce by N_2H_4 and had a significantly higher binding energy for the N_2/N_2H_4 and H_2/N_2H_4 peaks. The difference in N_2/N_2H_4 desorption temperature and the absence of one of the H_2/N_2H_4 binding states indicated a significant chemical difference between the two catalysts.

In the same apparatus flow experiments were performed by continuously injecting N_2H_4 (using a Sage syringe pump) and observing the products formed with the mass spectrometer. Also, aliquots of N_2H_4

were injected and the amount of each product formed was measured as a function of catalyst temperature.

The product stoichiometry was measured on the RRC catalyst as a function of catalyst temperature. At all conditions of temperature and flow rate complete reaction occurred. Below 573 K, NH_3 and N_2 were the only products, in a 4:1 ratio ($3N_2H_4 \rightarrow N_2 + 4NH_3$). Above 873 K, H_2 and N_2 were the only products, in a 2:1 ratio ($N_2H_4 \rightarrow N_2 + 2H_2$). A similar transition in product distribution was observed for ammonia decomposition over the same catalyst.

2. Surface Area Titration (SAT)

A new technique was developed for measurement of the surface area of Ir-crystallites on alumina and the results were correlated with those obtained from TPD. The procedure consists of reacting chemisorbed oxygen with carbon monoxide and measuring the amount of carbon dioxide produced. Only the Ir-metal sites (and not the support) will catalyze this reaction at room temperature in accordance with the stoichiometry

$$Ir\text{-}O + 2CO(g) \rightarrow Ir\text{-}CO + CO_2(g)$$

where Ir-O and Ir-CO represent chemisorbed oxygen and carbon monoxide, and the letter g stands for gas-phase species; therefore, such a surface titration provides quantitative information on the surface area of the catalyst.

The surface area results and the calculated average particle size are listed in Table 2. Also included in Table 2 are the surface areas for a RRC catalyst deactivated by sintering in H_2 and H_2O at 1473 K.

3. Auger Spectroscopy Surface Analysis (AES)

Five samples of Shell-405 catalyst representing fresh and used catalysts from RPL and RRC were examined in the Auger electron spectrometer in order to detect the buildup of surface contaminants on exposure to hydrazine. The Auger spectrometer is particularly useful in catalytic studies since it measures the chemical composition of the surface to a depth of the first few monolayers. The results of the AES study are summarized in Table 3.

For each sample the peak heights listed represent the elemental composition of the surface, normalized to the height of the oxygen 510 eV signal (from the Al_2O_3 support). The values are averaged over several different locations on the catalyst, since some spatial variation was observed. It can be seen that the surface composition changed substantially after exposure to N_2H_4. The spectra show the buildup of carbon, calcium, mercury, and nitrogen on the catalyst surface. These impurities were detected in the used samples provided by RRC and in the catalysts exposed to N_2H_4 in our laboratory. The deposition of calcium on the catalyst surface is most likely caused by impurities present in liquid hydrazine. The surface nitrogen results from hydrazine decomposition. This adspecies could not be removed by heating the catalyst in He to 1250 K (Sample No. 4). It is quite likely that the reduction in iridium surface area of Shell-405 caused by prolonged exposure to hydrazine is associated with the buildup of surface impurities on the iridium.

4. Discussion

The study of N_2H_4 decomposition on Shell-405 catalyst has yielded significant new information about the changes in catalyst surface properties after exposure to hydrazine. Each of these changes may lead to catalyst deactivation. The used catalysts exhibited (1) a decrease in reactive

surface area, and (2) a significant buildup of surface impurities. Because the binding energies of the adspecies, left behind on the catalyst after N_2H_4 exposure, did not change, we are led to conclude that the loss in active surface area is primarily due to the irreversible buildup of surface adsorbates. Among these species are the impurities present in the liquid hydrazine fuel. However, the formation of a strongly bound nitrogen adspecies on Shell-405 suggests an indigenous tendency of iridium toward the formation of nitridic-type surface compounds. After prolonged exposure to N_2H_4 it could become a major source of catalyst deactivation.

B. Mechanistic Studies of Heterogeneous Hydrazine Decomposition

1. Introduction

The purpose of this work is to establish the reaction paths and associated rates for elementary steps of importance in the operation of a hydrazine monopropellant thruster. This information is especially important for the following reasons:

- Establishment of catalyst activity for use in catalyst standardization, testing, and modeling.
- Understanding the mode of catalyst activity decay in order to minimize this effect.

Two types of experiments using a very low-pressure pyrolysis (VLPP) fused quartz reactor have been performed. In the first, a triple-aperture reactor (general details of the experimental set-up are given in reference 1) was employed to study hydrazine decomposition in the temperature range 700 K to 1300 K. At temperatures from 700 - 800 K a low activation energy ($\sim$13 kcal mole^{-1}) heterogeneous process was observed. A half-order heterogeneous reaction was found to predominate at the higher temperatures ($\gtrsim$ 825 K), precluding homogeneous rate determination. This mode of decomposition has been quantitatively analyzed.

In the second type of experiment, Shell-405 catalyst was placed directly into a fixed-aperture VLPP reactor, and the disappearance of N_2H_4, as well as the appearance of N_2 and NH_3 products, monitored over a wide temperature range (300 to 1100 K). The analysis was made possible through use of a recently constructed modulated-beam detection system. A number of heretofore unrecognized features of the decomposition have been observed. However, until we can confirm our measurements in a system free of catalyst deactivation, the results should be regarded as tentative.

Details of the experimentation in these two areas are given below.

2. Experimental Measurements on Quartz Surfaces

a. Experimental Details

These studies were originally intended for measuring the rate and determining the mechanism of the homogeneous decomposition of N_2H_4 in order to assess the role of the vapor-phase reaction in the operation of a monopropellant rocket thruster. This task turned out to be far more difficult than anticipated[2] because of sorption of N_2H_4 on the walls of the pyrex inlet system, the quartz reactor, and the stainless steel detection chamber. This "memory" effect perturbed the measurements as the N_2H_4 flow changed (by reaction or by change in total flow). For example, the time to reach steady-state flow decreased almost linearly with the flow rate. If the temperature changed so that the fraction of unreacted N_2H_4 changed from 1.0 to 0.5, the time to reach steady-state conditions was ~5 minutes at a flow of 2×10^{16} molecules sec^{-1} and ~50 minutes at a flow of 2×10^{15} molecules sec^{-1}.

In a series of runs designed to bypass this source of error, the hydrazine line flow rate and aperture were held constant and

the temperature was slowly varied during each run. Steady-state conditions were verified by holding the temperature constant for extended periods of time (one hour was typical). The gas stream leaving the reactor was chemically analyzed with a quadrupole mass spectrometer. Disappearance of the N_2H_4 mass spectral peak was always measured relative to premixed argon, the carrier gas, since the usual technique of obtaining the peak height ratio of reacted-to-total-reactant flow (using a reactor-bypass valve) proved unreliable because of adsorption effects in the inlet region.

At all but the highest flow rates, analysis of N_2 product was severely complicated by the presence of CO in the stainless steel detection chamber. Also, at these lower flows, product NH_3 analysis was impossible due to its affinity for metal surfaces. Consequently, in this flow regime ($\lesssim 10^{16}$ molecules sec^{-1}), reliable values for product concentration could not be obtained. However, at higher flows, the reaction produced quantities of NH_3 and N_2 as products consistent with the amount of N_2H_4 decomposed in accord with the reaction $3N_2H_4 \rightleftharpoons 4NH_3 + N_2$.

Two apparently different types of heterogeneous reactions were found to occur in this system.

b. Low-Temperature Reaction (575 - 925 K)

In the small-aperture reactor (~33,000 collisions $molecule^{-1}$), decomposition of N_2H_4 into N_2 and NH_3 was clearly observed in the above temperature range. The extent of reaction was somewhat dependent on the recent history of the reactor and varied between 0-50%. The order of reaction was difficult to accurately ascertain due to the variability of the rate and previously mentioned "memory" effects, but it is clear that the order is >0.5. Since adsorption problems would tend to make reaction appear to be of lower order, the data do not preclude a pure first-order reaction. In fact, other workers have reported such kinetics

on silica surfaces in this temperature range. If we assume first-order behavior, the value derived for the activation energy is ~13 kcal $mole^{-1}$ (at 675-725 K). This is in rough agreement with the value of Szwarc[3] of ~10 kcal $mole^{-1}$, and Hanratty et al.,[1] of 9.3-15.7 kcal $mole^{-1}$.

In contrast to the above-mentioned workers, we found that this rate levels off in the range 775-900 K and declines in the region 900-925 K. In particular, after heating from a lower temperature to the region near 900 K, the reaction rate appears unstable. By heating and cooling in this region or by switching temporarily to a larger aperture, the rate may be caused to decrease considerably (e.g., from 50 to 20% over a period of ~2 hours). This instability does not occur at lower (<875 K) or higher (>975 K) temperatures. As the temperature increases from 900 K, the high-temperature reaction path becomes more important and eventually predominates.

c. High-Temperature Reaction (825-1275 K)

At these higher temperatures, the decomposition of N_2H_4 was investigated using all three apertures (1, 3, and 10 mm in diameter) of the VLPP reactor. The results were analyzed on the basis of a half-order reaction. Using the relationship:

$$R_A = k_e[A] + k_{1/2}[A]^{1/2} = k_e[A]_o ,$$

the half-order rate constant is found to be:

$$k_{1/2} = \left(k_e f_r R_A\right)^{1/2} \frac{\left(1 - f_r\right)}{f_r} ,$$

where the terms are defined as:

$R_A \equiv$ flow of N_2H_4 into reactor per unit reactor volume (molecules cm^{-3} sec^{-1})

$k_e \equiv$ escape rate constant (sec^{-1})

$k_{1/2} \equiv$ escape rate constant (sec^{-1})

$[A] \equiv$ steady-state concentration of N_2H_4 (molecules cm^{-3})

$[A]_0 \equiv$ steady-state concentration of N_2H_4 at $k_{1/2} = 0$

$f_r =$ fraction of N_2H_4 remaining $= \dfrac{[A]_0 - [A]}{[A]_0}$

The variations of $k_{1/2}$ with temperature in terms of Arrhenius plots are displayed in Figures 1 a-c for three different apertures, and parameters derived from them are given in Table 1. Figure 2 shows $k_{1/2}$ versus flow rate at the representative temperature of 1025 K. Some noteworthy points are

(1) The leveling-off of the rate for the smallest aperture at lower temperatures, Figure 1-c, is due to the lower temperature reaction discussed previously.

(2) The apparently low Arrhenius parameters for the 1-mm aperture (Table 1), as well as the larger uncertainty of the measurement in this case, probably result from uncertainty due to the smaller temperature range over which these data were obtained.

(3) In Figure 2 note that, within experimental uncertainty, rates for the 1-mm and 3-mm aperture reactor are coincident and generally flow-independent. However, flow-dependent behavior apparently begins to occur for decomposition in the 10-mm aperture reactor experiments. At the lower flows in this reactor, neglecting the two high $k_{1/2}$ values at $\sim 1.8 \times 10^{15}$ molecules sec^{-1} (discussed later), first-order kinetics may be approached.

d. High-Temperature Decomposition Mechanism

Since it is clear that gas-phase radicals do not play a part in N_2H_4 decomposition in a fused silica reactor (see later in this section), we must invoke a mechanism in which the intermediates involved in the reaction are adsorbed on the surface. Following is such a general scheme:

$$N_2H_4(\text{gas}) \underset{k_d}{\overset{k_a}{\rightleftharpoons}} X_s + Y_s \qquad (1)$$

$$X_s \xrightarrow{k_1} \text{Products} \qquad (2a)$$

$$Y_s \xrightarrow{k_1'} \text{Products} \qquad (2b)$$

in which X_s and Y_s are bound surface species resulting from N_2H_4 dissociative adsorption. Two criteria are required for the above mechanism to yield half-order kinetics under steady-state conditions: (1) $[X_s]/[S] \lesssim 0.3$, i.e., the surface is sparsely covered. This condition is necessary over the pressure range of our experiments for the kinetics to be adequately described by a single order. (2) $k_1[X_s]$, $k_1'[Y_s] \ll 2k_a[N_2H_4]$. This is the requirement that reaction (2) be rate-limiting, so that half-order kinetics are obtained, i.e.,

$$\text{rate} = k_1[X_s] = k_1\left(\frac{k_a}{k_d}\right)[N_2H_4]^{1/2} \quad .$$

In the following discussion, k_1 is assumed equal to k_1'; therefore, $k_1[X_s] = k_1'[Y_s]$.

Let us examine condition (1). The fractional surface coverage, σ, for reaction (1) may be easily calculated if it is assumed that surface partition functions are equal to unity:[5]

$$\sigma = \left(\frac{[N_2H_4]}{f_{N_2H_4}} \right)^{1/2} 10^{-E_r/2\theta}$$

where f_r is the portion function of N_2H_4 ($\sim 10^{27}$ molecules$\cdot$cm^{-3}), E_r is the heat of reaction (1) express in cal mole^{-1}, and $\theta = 4.576T$ with T the temperature in K. At 1000 K and $[N_2H_4] = 10^{14}$ molecules cm^{-3}, where surface coverage is maximum for our experiments:

$$\sigma = 10^{-6.5 - E_r/9.15T}$$

and thus for $\sigma < 0.3$, $E_r > -55$ kcal mole^{-1}, this condition is easily fulfilled.

Figure 2 shows the range of consistency of half-order kinetics. Apparently, deviation from such kinetics begins to be noticeable for the large-aperture reactor at lower flows where $k_{1/2}$ becomes somewhat flow-dependent (i.e., first-order kinetics is approached). This behavior can be understood if $k_a \sim 10^2$ sec^{-1}. According to standard transition-state theory, at T = 1100 K, $k_a \sim 10^{1.5-E_a/\theta}$ sec^{-1}, assuming a "tight" transition state for adsorption (E_a is the energy of adsorption) and $k_a \sim 10^{4.7-E_a/\theta}$ sec^{-1} for a "loose" transition state. Thus, condition (1) is roughly met for either a tight transition state with $E_a \sim 0$ or a loose transition state with $E_a \sim 6$ kcal mole^{-1}. Note that in the preceding discussion two high values of $k_{1/2}$ at a flow of $\sim 2 \times 10^{15}$ molecules sec^{-1} were neglected.*

*These two high values for $k_{1/2}$ for the large-aperture reactor were obtained on initial heating in two separate experiments. The lower values at these flows were obtained after the initial heating period of each of these two experiments and were more reproducible. This indicates that k_a decreased and stabilized after conditioning, and the lower values may have simply been due to a decrease in the number of active sites (dehydration of silanol sites?) on heating above ~1100 K.

We will now show that the observed kinetics preclude the formation of gas-phase NH_2 species. If the walls are assumed to bring about the equilibrium

$$N_2H_4 \overset{K_{eq}}{\rightleftharpoons} 2NH_2 \qquad (3)(3)$$

and we assume the rate limiting step is

$$NH_2 \overset{k_1''}{\rightarrow} \text{Products} \qquad (4)(4)$$

then the rate is

$$k_1''\left[NH_2\right] = k_{1/2}\left[N_2H_4\right]^{1/2} k_1''\left(K_{eq}\left[N_2H_4\right]\right)^{1/2}. \qquad (5)$$

For reaction (4) to be the rate-limiting step, $k_1''[NH_2]^{1/2} \ll$ forward+backward reaction rate of equation (3); however, $k_1'' \gg k_e$ for step (4) to compete with the first-order escape of NH_2 from the reactor. If the latter condition did not hold, first-order kinetics would result.

Note also that if reaction (3) is to occur at all, it must be catalyzed by the walls. The homogeneous gas-phase bond scission path leading to NH_2 radicals would be slow under our experimental conditions due to the large degree of "fall-off" for N_2H_4 in the pressure range of these experiments. The reverse recombination reaction must of course be wall catalyzed (the wall acting as a "third" body).

The equilibrium constant K_e for reaction 1 may be computed from the data provided in references 6 and 7. It is found to be $K_{eq} = 10^{6.5}$ molecules$^{1/2}$ cm$^{-3/2}$ at 1100 K. Since $k_{1/2} = 10^{(14.9\pm1.10)-[(37.1\pm1.0)/\theta]}$ molec$^{1/2}$ cm$^{-3/2}$ sec^{-1} (these parameters are

from the medium aperture data), then from equation (5)

$$k_1 = 10^{1.1}\,\text{sec}^{-1} \text{ at } 1100\ \text{K} \quad .$$

Since

$$\frac{[NH_2]}{[\text{Products}]} = \frac{k_e}{k_1}$$

and k_e for the 10, 3, and 1-mm apertures equals 122, 12.5, and 0.838 sec^{-1}, respectively, the above ratio yields 10, 1.0, and 0.067, respectively. Thus, it is clear that for this model to be valid, essentially all products in the large aperture and a substantial fraction in the medium aperture reactor would have to be NH_2 radicals. This would not be consistent with the observed half-order kinetics, nor with the observation that the $[NH_2]/[NH_3] < 0.05$.* This model cannot be correct; NH_2 gas-phase radicals are not involved in this reaction.

Although we have not been able to directly measure homogeneous reaction rates for N_2H_4 decomposition, the results we have obtained are of value for the following reasons:

(1) They are useful in designing and understanding experiments of the type described in the next section, where reaction at high temperatures of N_2H_4 on the silica surface of the reactor may compete with decomposition on iridium.

(2) To the extent that silica resembles alumina, our experiments indicate that the decomposition of N_2H_4 on the support material of Shell-405 at low temperatures (<575 K) should be negligible. In modeling

*Separate experiments were performed to obtain this value. A reactor of collision number similar to that of the 10-mm aperture reactor was used in conjunction with a modulated-beam detection system. No NH_2 radicals were seen using low electron energy (<25 eV) relative to product NH_3.

the high-temperature reaction of N_2H_4 in a catalyst bed, attention should perhaps be paid to the role of the alumina support in generating surface species that may migrate to the metal catalyst.

3. Experimental Measurements on Shell-405 Catalyst.

In a preliminary series of experiments, the decomposition of N_2H_4 on Shell-405 catalyst (iridium supported on alumina) has been studied. To obtain unambiguous results over a range of flow rates, and to be able to accurately measure product concentrations, a new detection system for a VLPP fixed-aperture reactor was utilized. In this system, the flow from the reactor volume was formed into a beam, the beam was modulated by a mechanical chopper and detected with a quadrupole mass spectrometer, and the modulated signal was selectively amplified through a lock-in amplifier. This ensured that the intensity of the measured mass-spectral signal directly reflected the concentration of the corresponding gas-phase species in the reactor.

Five pellets of unused Shell-405 catalyst were inserted into a 25-cm^3 fixed-aperture fused quartz reactor (effective outlet area = 1.22 mm^2). The average collision number of an unreactive species entering the reactor with the catalyst's external surface was 20 collisions $molecule^{-1}$. This average collision number will be essentially the same for even a reactive species if the reactivity is low enough so that concentration of this species is uniform in the reactor. This condition was basically satisfied in these experiments. The pressure was always in the molecular flow regime ($<5 \times 10^{-3}$ torr). Most experiments were carried out by varying the temperature between 300 and 1075 K (the reactor and catalyst are heated together) and measuring mass peaks associated with N_2H_4, NH_3, and N_2 under constant flow conditions.

The independence of the room temperature N_2H_4 decomposition rate with flow is illustrated in Figure 3. In this figure I_n represents

the intensity (arbitrary units) of the mass-spectral peak corresponding to m/e = n. Thus, the ordinate roughly corresponds to the inverse of the decomposition rate. Over the flow range 7×10^{15} - 1.4×10^{16} molecules sec^{-1}, corresponding to pressures 1.5×10^{-4} - 3×10^{-3} torr, the reaction rate was first order with respect to N_2H_4. This gives us some confidence that our results may be extrapolated up to engine operating conditions. All other runs were carried out at a flow of 1.4×10^{16} molecules sec^{-1}.

Figure 4 shows the dependence of relative product distribution as a function of temperature for the first run subsequent to Shell-405 insertion in the reactor. The erratic behavior of the decomposition on initial heating was found to be a generally observed phenomenon for each day's run. However, the behavior during subsequent cooling and heating was much more reproducible. Since no H_2 was seen at room temperature, the difference between the relative product distribution of its initial value (at point--begin) and its final value (at point--end) must have been due to relative changes in detection sensitivity.

Relative product distribution curves are given for different runs in Figures 5a-c. These values were obtained after initial heating of the reactor above 675 K. The general trend is clear. From about 300 - 425 K the products are NH_3 and N_2 only. This is inferred from the lack of H_2 (m/e = 2) even in the unmodulated signal at these temperatures. Over the range 325 - 775 K the reaction stoichiometry changes to one yielding largely N_2 and H_2. But, even at these high temperatures ~55% of the NH_3 remains undecomposed. Anomalous quantities of NH_3 were evolved in the range ~425 K. This effect is especially apparent in Figure 5c, where several measurements were made in this temperature region and where it was found that the quantity of NH_3 evolved depended on the previous treatment of the catalyst. This effect is assumed to be due to desorption of NH_3 from Shell-405 at this temperature (see Section A1). As the temperature was increased from

575 to 675 K, large quantities of N_2 evolved from the catalyst (see Section A1).

However, no large change occurred in the amount of unreacted N_2H_4 when the temperature was increased from 300 - 675 K (Figure 6). This very interesting result indicates that only the reaction stoichiometry and not the activity changes in this range of temperature, i.e., the apparent activation energy for the N_2H_4 decomposition process is zero. The decomposition has not yet been studied carefully enough at higher temperatures to give a firm quantitative idea of the change in activity in this region. It is certain, however, that a gradual activity increase occurs with temperature above 775 - 875 K.

Finally, Figure 7 shows the calculated activity of Shell-405 over the period in which runs were carried out. It should be mentioned that catalyst activity, as we have discussed it, differs from conventional definitions of the quantity.[8] Generally, catalyst activity is used to mean activity per unit of total active surface area. Our measurements yield directly the activity per external surface area. For as active a catalyst as Shell-405, this is a more meaningful parameter to use to understand its diffusion-controlled reactions in a thruster. A large part of the total surface area may play no role in the reactivity of the catalyst pellets with the catalyst bed.

The decrease in activity of ~40% (Figure 6) over the eleven days of experiments is probably due to a mode of poisoning not associated with the N_2H_4 decomposition itself. The effect may be due to irreversible adsorption of contaminants present in the reactor. However, the consistency of activity over the first three days indicates that N_2H_4 decomposes on unpoisoned Shell-405 once every 50 collisions with the external surface.

These data are preliminary in nature and must be viewed with caution until we can confirm them in future experiments. A possibility

exists that the silicone stopcock-grease present in the inlet system and the silicone pump oil in the pumping chamber may have poisoned the external surface of the catalyst before any runs were performed. In that case, our data would reflect the decomposition of N_2H_4 within the pellet, i.e., for molecules experimenting at least several collisions within the pellet. A greaseless inlet system and cryo-trapped pumping chamber are now under construction for elimination of these possible problems and for a further examination of the kinetics of the N_2H_4 decomposition on unused catalyst.

4. Conclusions

a. Decomposition of N_2H_4 on SiO_2-surfaces

(1) At temperatures 575-775 K, N_2H_4 decomposes on fused silica in an assumed first-order process with an activation energy ~13 kcal $mole^{-1}$. The rate of this decomposition levels off from 775-875 K and begins to decrease in the range ~875-900 K.

(2) At high temperatures ($\gtrsim$ 975 K) and low pressures ($<10^{-2}$ torr), N_2H_4 undergoes half-order decomposition on fused silica with an activation energy slightly greater than half of the N-N bond dissociation energy. The best value for this rate constant is $10^{(14.9\pm1.0)-[(37.1\pm1.0)/\theta]}$ $molecules^{1/2}$ $cm^{-3/2}$ sec^{-1}.

b. Decomposition of N_2H_4 on Shell-405 Catalyst

(1) The low-pressure flow reactor (i.e., VLPP) technique has been shown to be an unambiguous experimental method for the investigation of Shell-405 catalyst activity and the kinetics of its decomposition of N_2H_4.

(2) Preliminary experiments have clarified several aspects of the nature of N_2H_4 decomposition on fresh Shell-405. The major points are:

(a) This reaction obeys first-order kinetics over the range 1.5×10^{-4} to 3×10^{-3} torr.

(b) At low-temperatures (300-425 K) decomposition products are entirely NH_3 and N_2, while at high temperatures (~675-1075 K) ~45% of the NH_3 is decomposed to N_2 and H_2. This value is somewhat less than is found in the exhaust of a real monopropellant thruster (66% ammonia dissociation is reported for a 5-lb thruster operating at ~1175 K.[9] The difference may be due to NH_3 decomposition downstream in the catalyst bed.

(c) No appreciable change in activity for N_2H_4 decomposition is observed from 300 to ~775 K.[10] This agrees with the work of Smith and Solomon on a monolithic alumina-supported iridium catalyst over a range of 350-750 K.

(d) One out of fifty collisions of N_2H_4 with the external catalyst pellet surface is effective in decomposition.

REFERENCES

1. D. M. Golden, G. N. Spokes, and S. W. Benson, Angew. Chem. (Internat. Edit.) 12, 534 (1973).

2. S. W. Benson, et al., AFOSR Summary Report, Contract No. F44620-73-C-0069, April 1974.

3. M. Szwarc, Proc. Roy. Soc., A.198, 267 (1949).

4. T. J. Hanratty, J. N. Patterson, J. W. Clegg, and A. W. Lemmon, Jr., Ind. Eng. Chem., 43, 1113 (1951).

5. J. M. Thomas and W. J. Thomas, Introduction to the Principles of Heterogeneous Catalysis, Academic Press, New York (1967).

6. JANAF Thermochemical Tables, Dow Chemical Company, Midland, Michigan (1968).

7. S. W. Benson, Thermochemical Kinetics, John Wiley and Sons, Inc., New York (1968).

8. C. N. Satterfield and T. K. Sherwood, The Role of Diffusion in Catalysis, Addison-Wesley Co., Reading, Massachusetts (1963). Chapter 3.

9. B. W. Schmitz and W. W. Wilson, AF Final Report, AFRPL-TR-71-103 (1971).

10. O. I. Smith and W. C. Solomon, AF Final Report, AFRPL-TR-73-103 (1973).

Table 1

SURFACE PROPERTIES OF SHELL-405 CATALYSTS*

Property	Catalyst Sample	
	RPL	RRC
Mesh size	14-18	25-30
Surface area (m^2/g Ir)	64.2	51.4
Average Ir-crystallite diameter (Å)	41	52
Surface population (molecules/g cat.) x 10^{19}		
H_2/N_2H_4	11	8
N_2/N_2H_4	2	1.5
NH_3/N_2H_4	15.5	9.7
Peak TPD temperature (K)		
N_2/N_2H_4	733	663
H_2/N_2H_4	733	448;673

*Catalysts reduced in H_2 (1 atm) at 557 K for 2 hours.

**Heating rate for TPD = 2 Ks^{-1}.

Table 2

SURFACE PROPERTIES OF FRESH AND USED
SHELL-405 CATALYSTS

Property	RPL		RRC		
	Fresh	Used*	Fresh	Used**	Sintered†
Surface area (m^2/g Ir)	64.2	61.4	51.4	27.5	24.6
Ave. Ir-crystallite diam. (Å)	41	43	52	97	108
Peak TPD temperature‡ (K)	733	-	663	663	663

* After a total of 900-sec exposure to hydrazine during 125 cold starts in rocket thruster.

** After exposure to 1097 moles hydrazine in pulse mode rocket thruster operation.

† After exposure to steam/hydrogen at 1475 K for 15 minutes.

‡ Heating rate for TPD = 2 Ks^{-1}.

Table 3

SURFACE STUDY OF SHELL-405 BY AUGER ELECTRON SPECTROSCOPY

Surface Element (Peak Energy, eV)	Relative AES Peak Heights				
	#1	#2	#3	#4	#5
Ir (51)	0.51	0.52	0.47	0.86	0.58
Ir (229)	0.03	0.015	0.04	0.066	0.025
C (272)	- -	0.041	0.09	0.11	0.07
Ca (291)	- -	0.052	0.03	0.07	- -
Hg (76)	- -	0.15	0.26	0.14	- -
N (281)	- -	0.028	0.012	0.028	- -

#1 Fresh catalyst from Rocket Research Corporation (RRC).

#2 Used catalyst from RRC. Each gram of catalyst had been exposed to 1097 moles N_2H_4 in a rocket thruster.

#3 Fresh RRC catalyst. Each gram was exposed to 1.1 moles N_2H_4 in our laboratory at catalyst temperatures from 300 to 725 K. Also, the catalyst had been subjected to several high temperature flashes up to 1075 K.

#4 Used catalyst from RRC exposed to a series of temperature-programmed desorption experiments. The catalyst was heated in helium to 1250 K before placement in the Auger system.

#5 Fresh catalyst from Rocket Propulsion Laboratory, Edwards AFB.

Table 4

ARRHENIUS PARAMETERS FOR HYDRAZINE DECOMPOSITION ON FUSED SILICA

Aperture Diameter (mm)	A-Factor (10^{-14} molecules$^{1/2}$ cm$^{-3/2}$ sec^{-1})	Activation Energy (kcal mole^{-1})
10	13 ± 6	38.1 ± 1.0
3	7.4 ± 2.0	37.1 ± 1.0
1	3.0 ± 1.5	36.0 ± 3.0

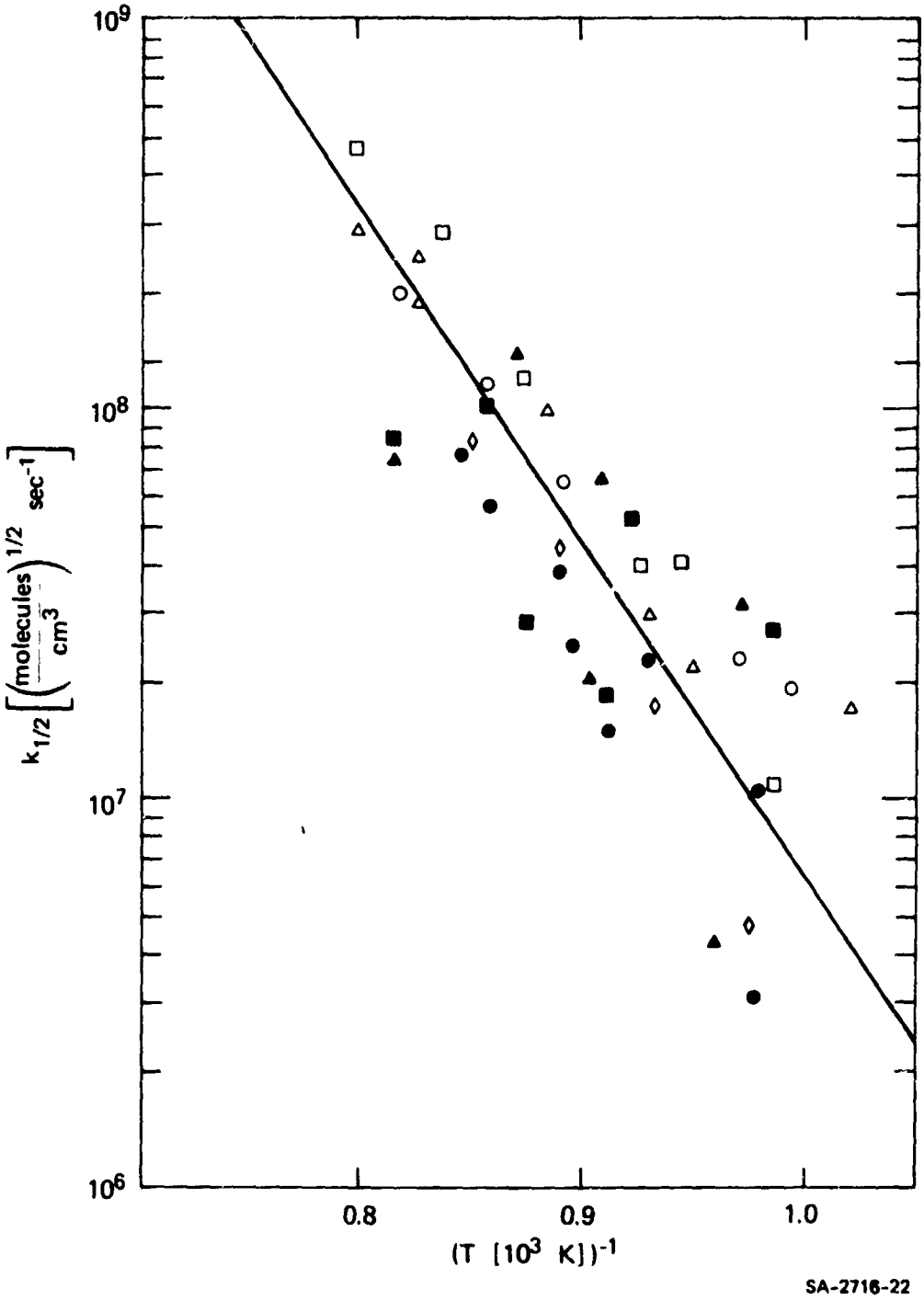

FIGURE 13 ARRHENIUS PLOTS FOR DECOMPOSITION OF HYDRAZINE IN A QUARTZ, TRIPLE-APERTURE, VLPP REACTOR

(a) Measurements with 176 collisions molecule^{-1} reactor Flow (10^{15} molecules sec^{-1})
□ - 20; △ - 16; ○ - 11; ◊ - 7.7, ■ - 1.9; ♦ - 1.8, ▲ - 1.4

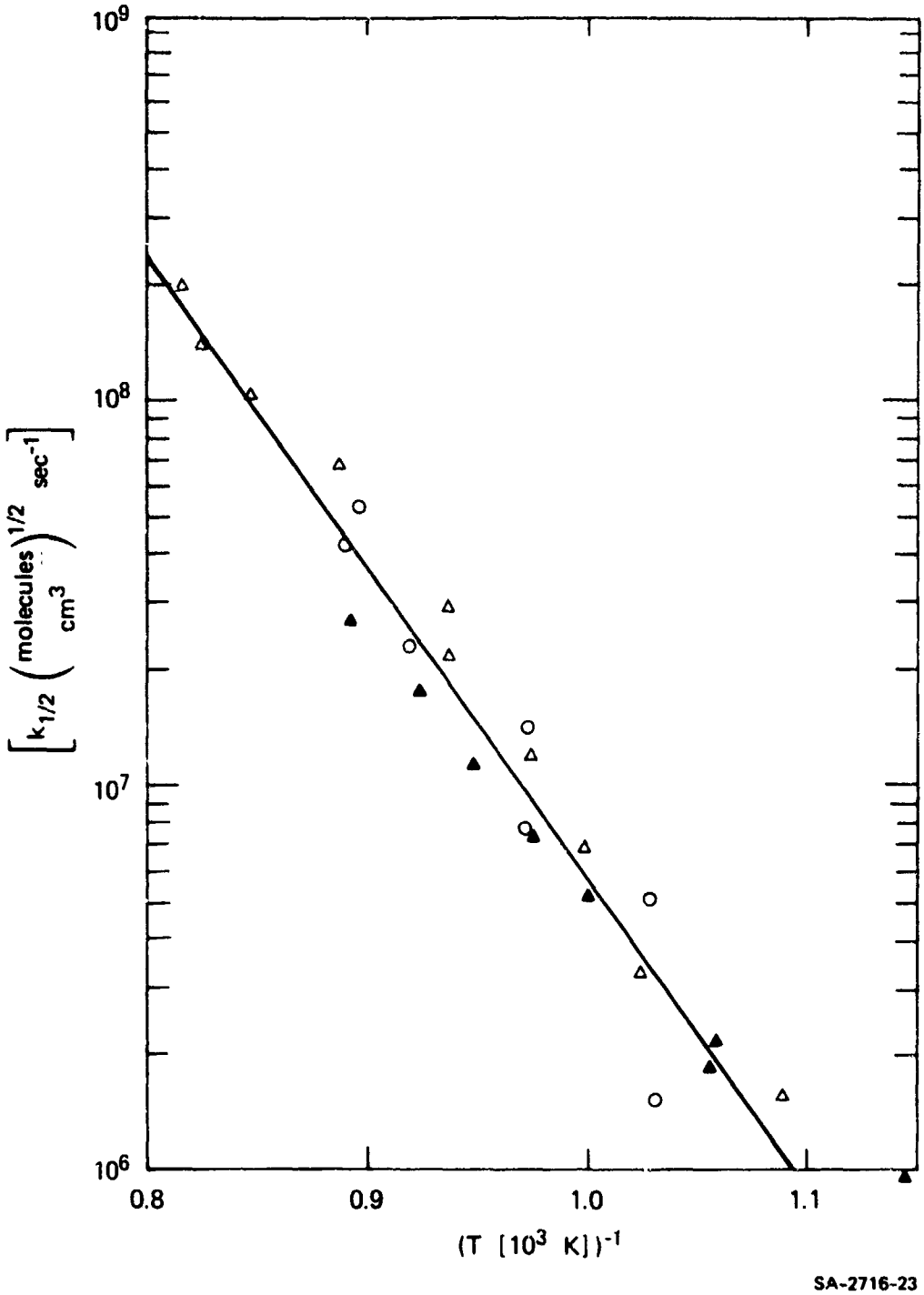

FIGURE 1b ARRHENIUS PLOTS FOR DECOMPOSITION OF HYDRAZINE IN A QUARTZ, TRIPLE-APERTURE, VLPP REACTOR

(b) Measurements with 1930 collisions molecule^{-1} reactor: Flow (10^{15} molecules sec^{-1}) △ - 18; ○ - 8.8; ▲ - 1.9

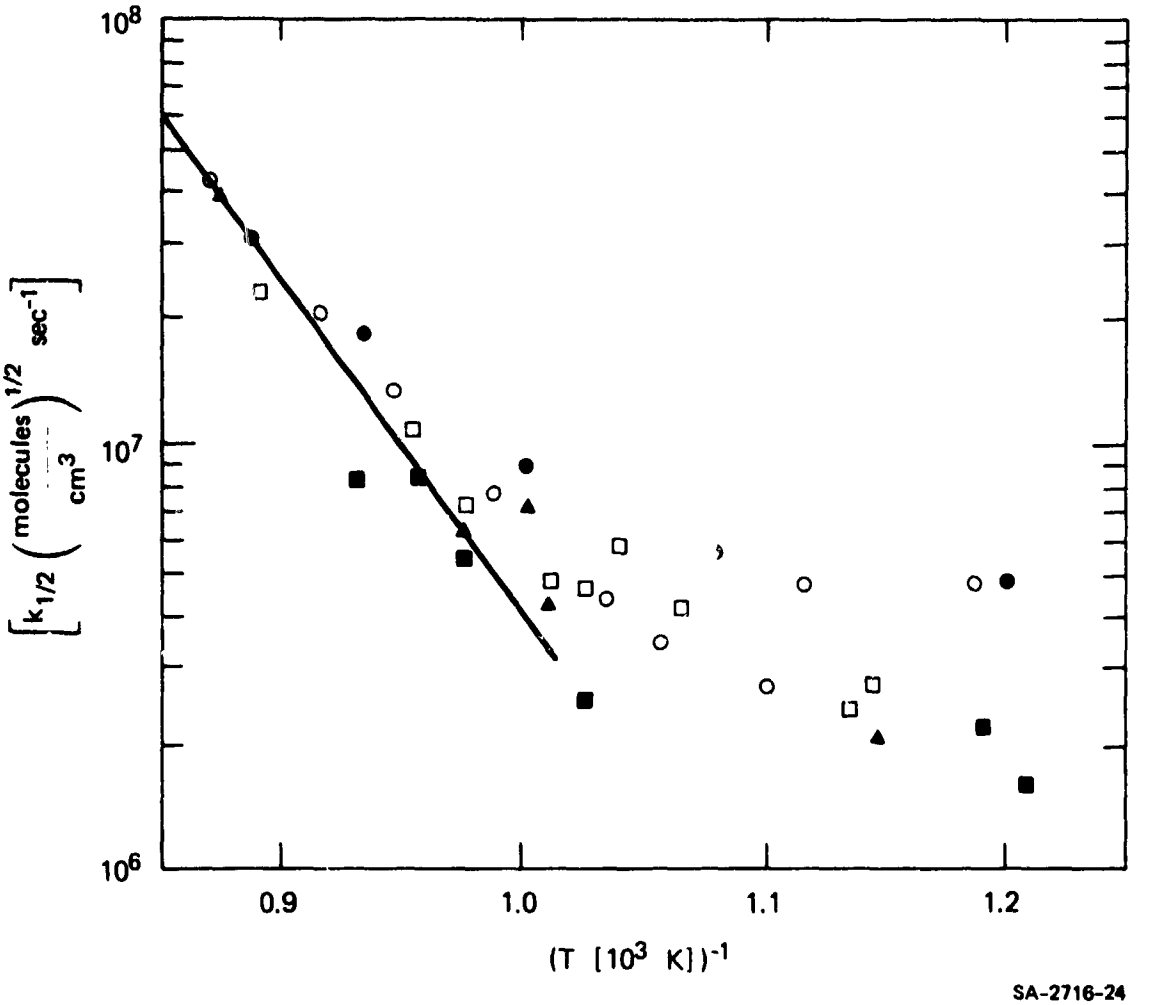

FIGURE 1c ARRHENIUS PLOTS FOR DECOMPOSITION OF HYDRAZINE IN A QUARTZ, TRIPLE-APERTURE, VLPP REACTOR

(c) Measurements with 2.7×10^3 collisions molecule^{-1} reactor: Flow (10^{15} molecules sec^{-1})
● - 15; ○ - 4.6; □ - 2.1; ▲ - 1.5; ■ - 1.4

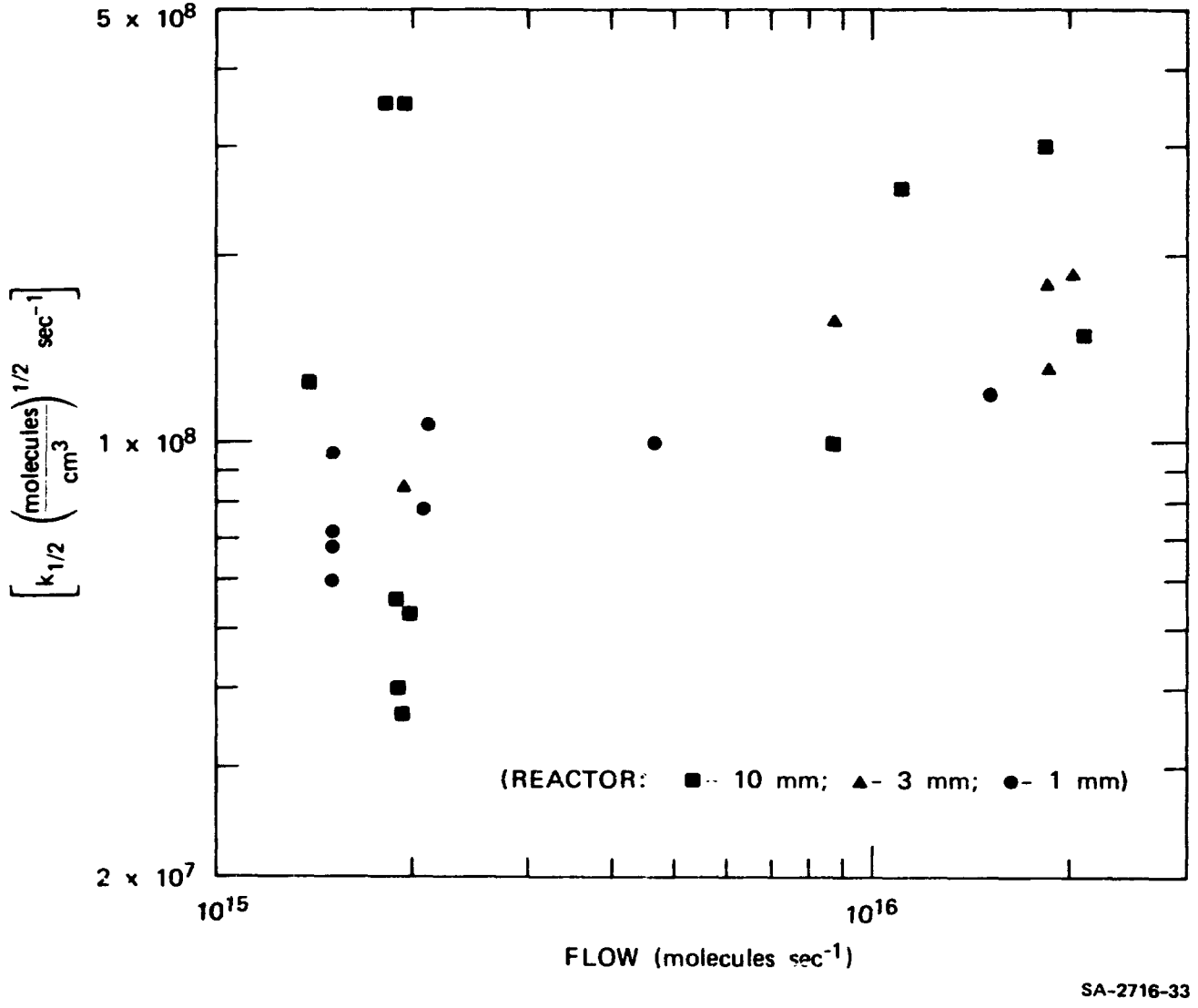

FIGURE 2 PLOT OF HALF-ORDER RATE CONSTANTS AS A FUNCTION OF FLOW FOR THREE APERTURE SIZES AT 1025 K FOR THE DECOMPOSITION OF N_2H_4 ON FUSED SILICA

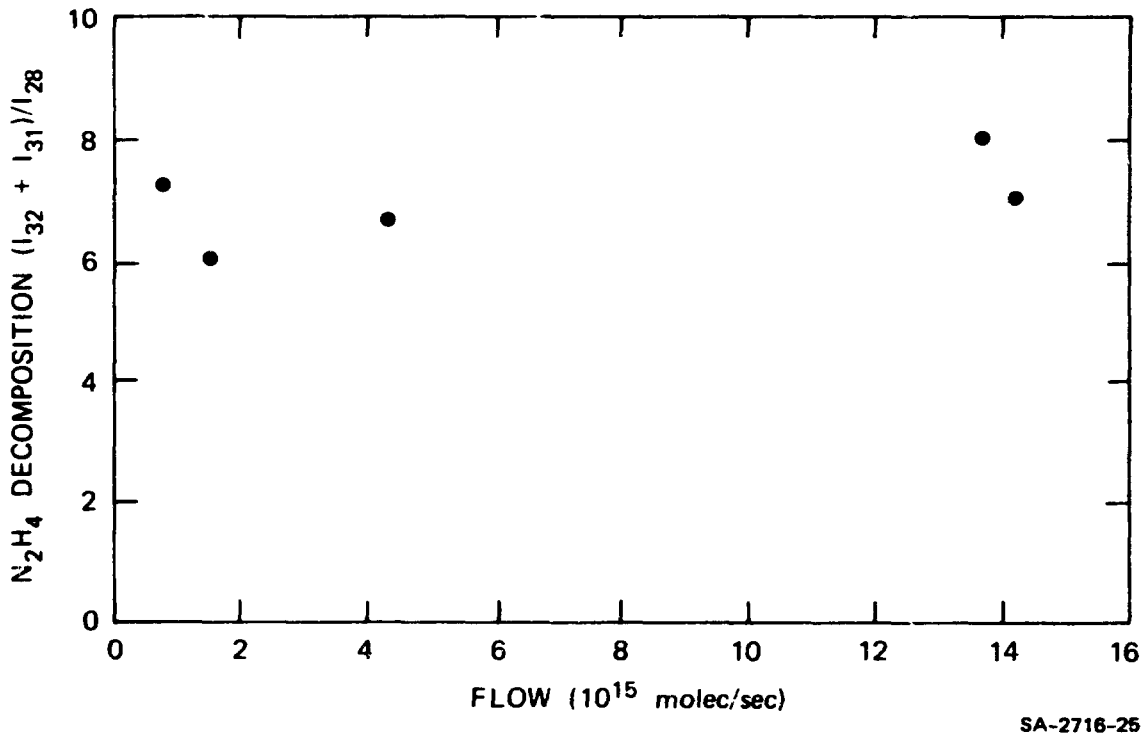

FIGURE 3 MEASURE OF N_2H_4 DECOMPOSITION ON SHELL-405 AS A FUNCTION OF FLOW RATE

I_n = intensity of mass-spectral peak, corresponding to n = m/e.

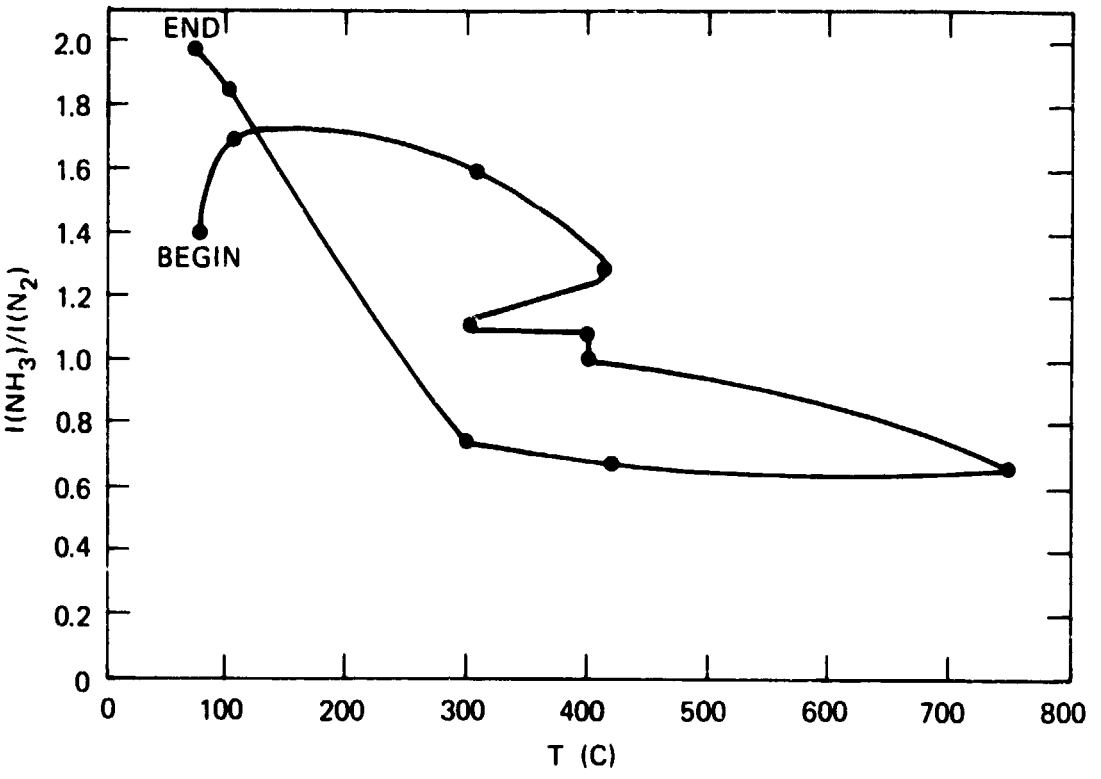

FIGURE 4 VARIATION OF NH_3/N_2 SIGNAL INTENSITY RATIO WITH TEMPERATURE OF REACTOR CONTAINING SHELL-405

This was the first run after the new pellets were placed in the reactor.

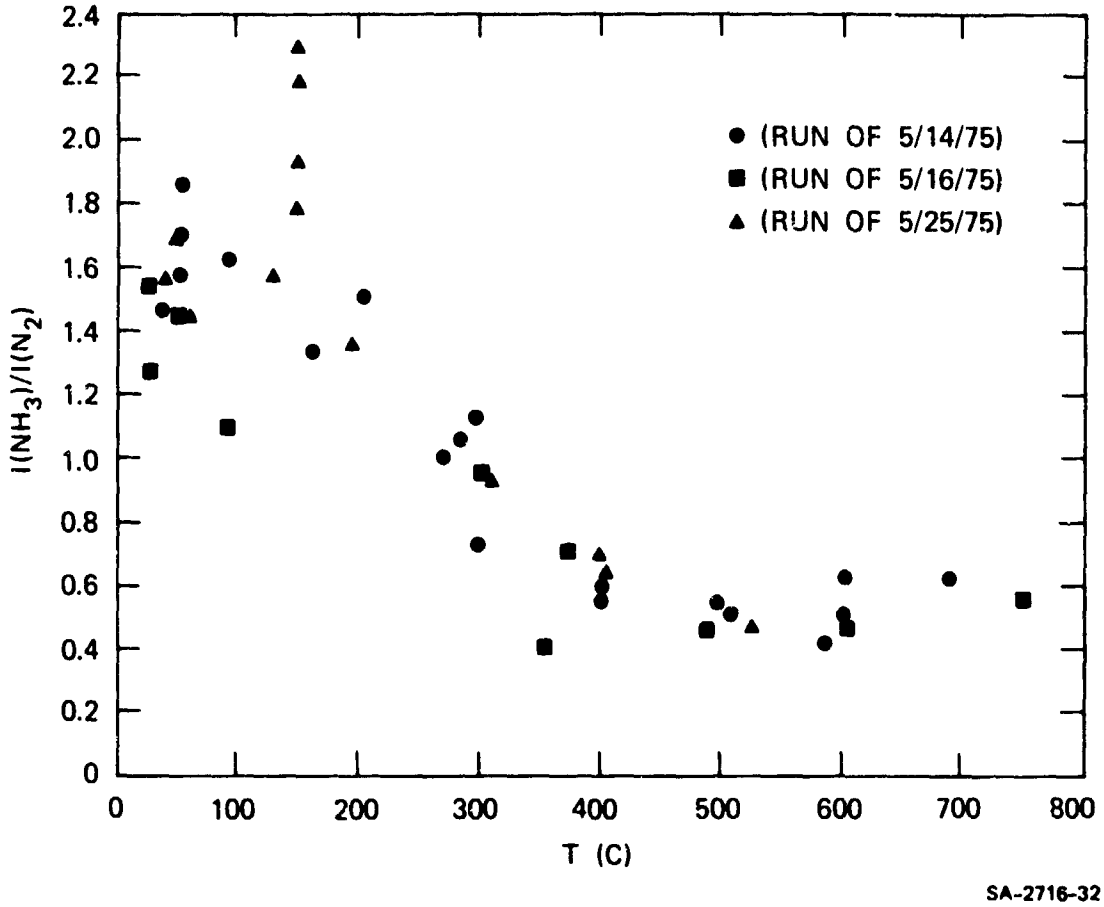

FIGURE 5 VARIATION OF NH_3/N_2 SIGNAL INTENSITY RATIO WITH TEMPERATURE OF REACTOR CONTAINING SHELL-405 UNDER AN INFLUX OF N_2H_4 OF $\sim 10^{16}$ MOLECULES SEC^{-1}

These data were obtained after initial heating of the reactor (and catalyst) above ~675 K.

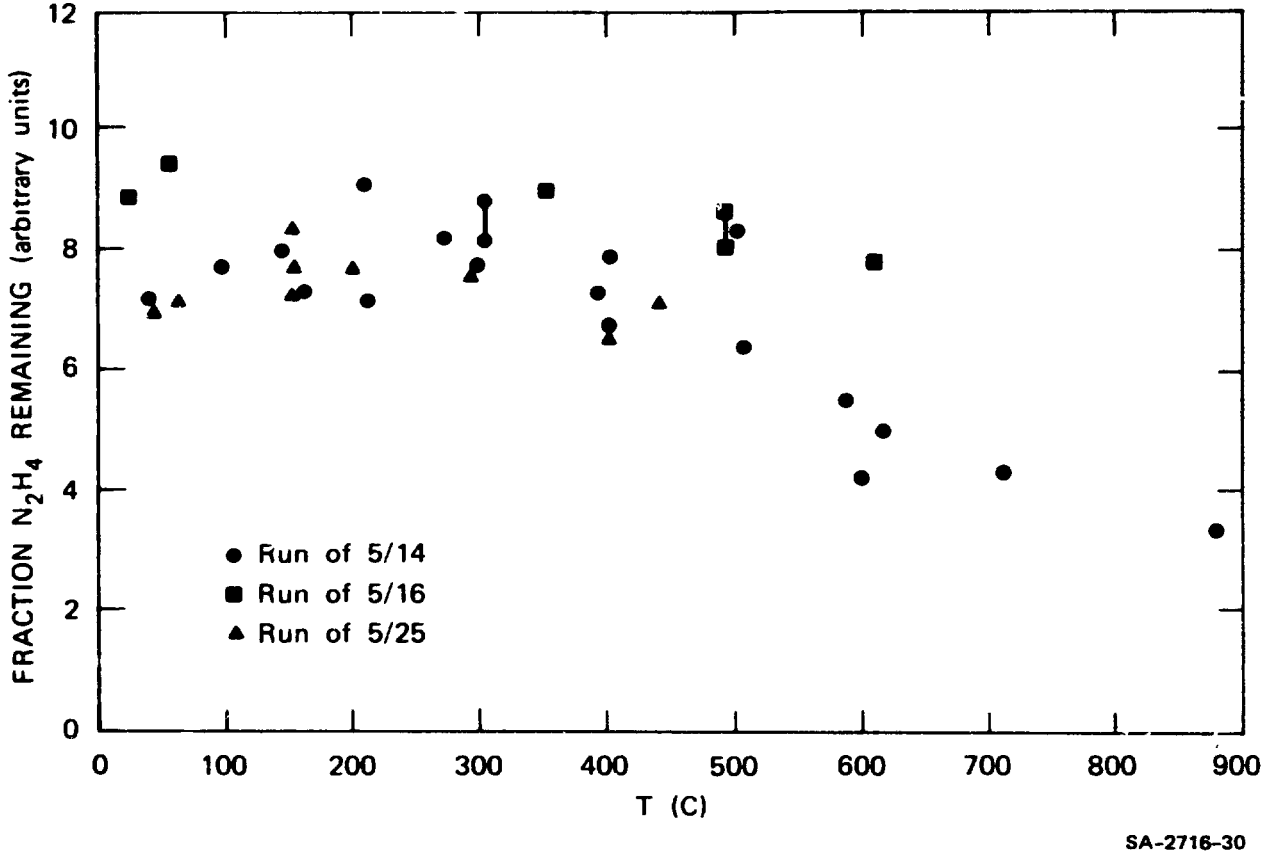

FIGURE 6 FRACTION OF N_2H_4 UNREACTED OVER FIVE SHELL-405 PELLETS AS A FUNCTION OF TEMPERATURE FOR A NUMBER OF DIFFERENT RUNS

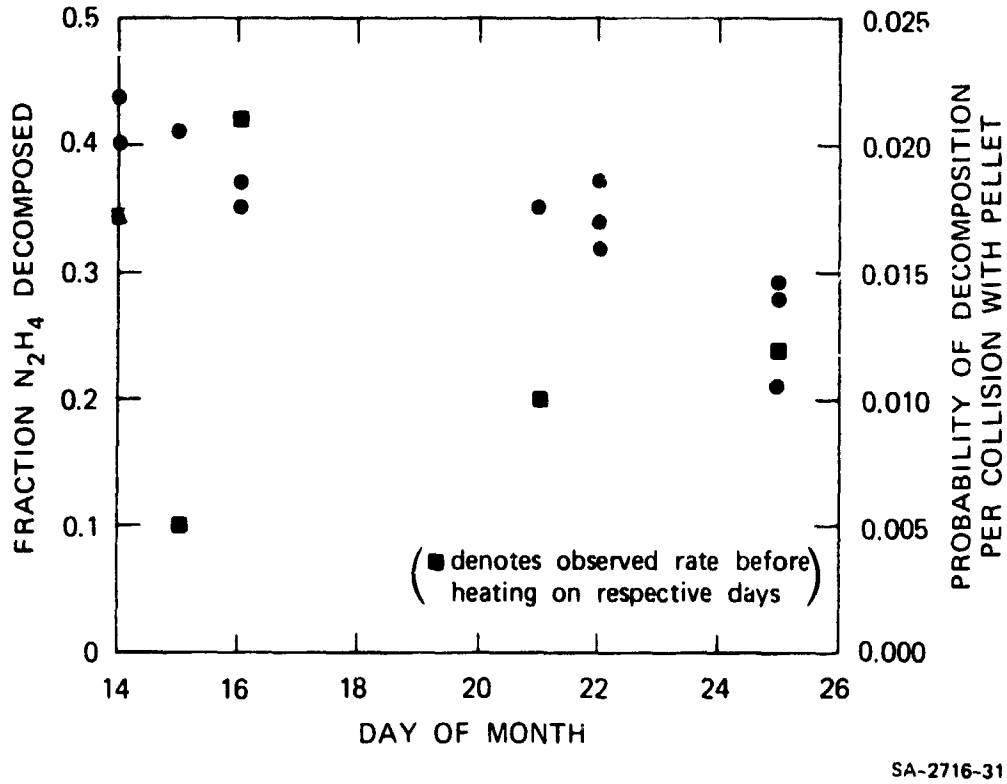

FIGURE 7 FRACTION OF N_2H_4 DECOMPOSED OVER FIVE SHELL-405 PELLETS AT 300-315 K OVER THE PERIOD OF EXPERIMENTATION

Appendix A

TEMPERATURE-PROGRAMMED DESORPTION SPECTROSCOPY OF N_2H_4 DECOMPOSITION ON Al_2O_3-SUPPORTED Ir CATALYST

TEMPERATURE-PROGRAMMED DESORPTION SPECTROSCOPY OF N_2H_4 DECOMPOSITION ON Al_2O_3-SUPPORTED Ir CATALYST*

John L. Falconer and Henry Wise
Solid State Catalysis Laboratory
Stanford Research Institute
Menlo Park California 94025

Abstract

At room temperature the steady-state decomposition of N_2H_4 over an alumina-supported Ir-catalyst was found to yield NH_3 and N_2 while at temperatures above 800 K the products were N_2 and H_2. Following exposure of the catalyst surface to N_2H_4 the adsorbed species were studied by the temperature programmed desorption technique at a heating rate of 2 K s^{-1}. The desorption products included N_2, NH_3 and H_2 originating from different binding states. For the more strongly bound nitrogen [$N_2(\beta_2)$] the kinetics of desorption following exposure to N_2H_4 are of first-order with a desorption rate constant of $3 \times 10^7 \exp(26{,}800/RT)$ s^{-1}. Adsorption of oxygen on the iridium catalyst was found to decrease the nitrogen binding energy and increase the nitrogen coverage. The surface coverage of all adsorbed species was found to be significantly smaller on catalysts that had been used in pulsed mode fuel thrusters. The differences observed were correlated with the loss in metal surface area of the catalyst. However, no differences in the binding energies of the various adspecies were detectable between fresh catalyst and used catalyst.

---

*Support of this research by the Air Force Office of Scientific Research (Contract No. AFOSR F44620-73-C-0069) is gratefully acknowledged.

A. Introduction

In a preceding study[1] of hydrazine decomposition on the surface of polycrystalline iridium it was noted that strongly bound adsorbed species were formed, particularly chemisorbed nitrogen, that led to a gradual reduction of the catalytic activity of the Ir-ribbon. In the present study this work is extended to finely dispersed Ir-crystallites on an alumina support (Shell-405), as currently used for catalytic decomposition of N_2H_4 in monopropellant thrusters. To elucidate the nature of the surface adsorbate, we carried out temperature programmed desorption (TPD) spectroscopy after exposure of the powdered catalyst to aliquots of hydrazine in a microreactor. Shell-405 is particularly amenable to study by this experimental approach because of its high metal weight loading and relatively large Ir-surface area. Analysis of the experimental data permits identification of adsorbed species, their binding state on the surface, and their relative surface coverage. Also, our work on Shell-405 allows comparison with an alumina-supported Ir-catalyst prepared by Contour and Pannetier[2].

The purpose of our work is twofold: (1) to elucidate the causes of catalyst activity loss that occurs in operational monopropellant thrusters, and (2) to determine the mechanism of heterogeneous decomposition of hydrazine on the supported iridium catalyst.

A shorthand notation is adopted for describing the origin of each desorbing gas during TPD. The term A(x)/B(T) refers to desorption of the x-state of gas A following adsorption of gas B at temperature T (°C). For adsorption studies carried out at room temperature, the temperature designation is omitted from the notation.

B. Experimental Details

The apparatus was designed for continuous or pulsed flow studies, and for TPD experiments following exposure of the catalyst to reactants. The catalyst sample (0.1 g) was placed on a vycor frit contained in a vycor reactor (1 cm O.D.). The carrier gas, helium or argon, flowed continuously through the reactor at atmospheric pressure at a flow rate of 100 cm^3/min, corresponding to a catalyst contact time of about 6×10^{-2} s. The reactor was heated electrically by means of a nichrome-wound quartz tube placed around it. The catalyst temperature was measured by a chromel-alumel thermocouple in contact with the catalyst. The thermocouple wires (0.005" diameter) led from the reactor to a feedthrough and a recording instrument. While heating rates (β) of 0.2 to 4 Ks^{-1} were obtainable with this arrangement, most TPD experiments were performed at 2 Ks^{-1}. After leaving the reactor the products resulting either from steady-state decomposition or from TPD were continuously analyzed by mass spectrometry (EAI quadrupole mass spectrometer). For this purpose a small fraction of the gas stream leaving the reactor was leaked through an adjustable orifice into the differentially pumped mass spectrometer system operating at a total pressure of 10^{-6} torr. For TPD studies the supply of reactant was shut off while the inert carrier gas continued flow through the reactor. After attainment of the "background" gas composition the temperature of the catalyst was raised linearly at a prescribed heating rate. Quantitative analysis of the desorption products as a function of catalyst temperature was carried out by simultaneous recording of the mass spectrometer signal and the thermocouple output.

To obtain an absolute measure of the degree of surface coverage with the various adspecies during TPD and the product stoichiometry during flow experiments, it was necessary to calibrate the mass

spectrometer. Empirical calibrations for NH_3, N_2 and H_2 were obtained by injecting known amounts of each of the gases into the carrier stream flowing through the reactor and observing the total signal detected by the mass spectrometer.

Hydrazine was admitted by injecting a pulse of the liquid (0.01 to 10 μl) through a septum into the reactor, which was continuously swept by the helium stream. In continuous flow experiments N_2H_4 was fed through the septum from a gastight syringe, using a Sage syringe pump to maintain constant mass flow. A small auxiliary nichrome heater kept the inlet portion of the reactor wall sufficiently warm to vaporize the hydrazine so that only vapor contacted the catalyst. A similar procedure was used in experiments with water. Other gases (NH_3, N_2, H_2, O_2) were introduced into the reactor either by continuous flow from a storage cylinder or by injection of small pulses through the septum using a gastight syringe.

To obtain reproducible TPD spectra it was found necessary to reduce the Shell-405 iridium catalyst by exposure to several doses of 5 μl N_2H_4 at room temperature followed by heating to 800°C. The TPD studies were then carried out on the reduced catalyst after varying amounts of liquid N_2H_4 or gaseous NH_3 or H_2 had been injected to obtain different levels of surface coverage.* After the mass spectrometer signals had returned to their background levels, the catalyst was subjected to a prescribed heating cycle and the products were monitored as a function of catalyst temperature.

The iridium surface areas on the catalysts were measured by "surface titration", similar to that used for platinum[3], employing the reaction of chemisorbed oxygen with gaseous carbon monoxide. Oxygen was adsorbed at atmospheric pressure and 25°C after catalyst reduction in H_2 at 300°C

*Approximately 1 μl of liquid N_2H_4 or 250 μl of gaseous NH_3 or H_2 were sufficient to yield saturation coverage.

for 2 hours and cooling in He to room temperature. Pulses containing known amounts of carbon monoxide in helium were passed over the catalyst. The oxygen adatoms on the Ir sites react to form CO_2. Pulsing of CO was continued until no further sorption of CO occurred. Gas chromatographic measurements of the total CO_2 formed allow calculation* of the iridium surface area.[4]

The Shell-405 catalyst contained 32 wt% iridium on a low surface area alumina. Catalyst samples were obtained from Rocket Research Corporation (RRC) in Redmond, Washington. Comparison was made between the fresh RRC catalyst (A) and the used RRC catalyst (B), which had been exposed to a total of 1097 moles N_2H_4 per gram of catalyst in pulse-mode operation of a rocket thruster. The fresh catalyst had a particle size distribution equivalent to 25-30 mesh, while the used catalyst was in the size range of 30-35 mesh because of particle breakup in the thruster.

Hydrazine (Anhydrous-Technical grade from Olin Chemicals), containing three percent water, was used in the initial studies. However, most of the data were obtained with specially purified anhydrous N_2H_4 (obtained from Martin-Denver).† Mass spectrometer analysis indicated the presence of less than one percent water and no other detectable impurity. All gases used in our studies were of high purity, and were used directly from the cylinders without further purification.

---

*The ratio of oxygen atoms sorbed per surface Ir atom needs to be known to convert the mass of CO_2 produced to the number of Ir-surface atoms. In our calculations we use O/Ir = 1/2, based on separate adsorption studies.

†We are grateful to Lawrence William, who kindly supplied the purified N_2H_4.

C. Results

1. Desorption Studies with Fresh Catalyst (Shell-405)

After the reduced catalyst (A) had been exposed to hydrazine, it was subjected to TPD, and the concentration of each gaseous product leaving the solid surface was recorded. Figure 1 shows the mass peaks due to N_2, H_2, NH_3, and H_2O following N_2H_4 exposure sufficient to produce saturation coverage. No other desorption products were detected, and no unreacted N_2H_4 desorbed from the surface. At saturation coverage the N_2/N_2H_4 consisted of a single peak $N_2(\beta_2)$ with a peak temperature of 390°C; the H_2/N_2H_4 exhibited a broad peak at 140°C [$H_2(\alpha)$] and a $H_2(\beta)$ peak at approximately 400°C; and the NH_3/N_2H_4 desorbed in two very broad peaks located at 140°C [$NH_3(\alpha)$] and 355°C [$NH_3(\alpha_2)$]. The H_2O/N_2H_4 desorption consisted of a very small but broad peak extending to very high temperatures, characteristic of water desorption from the Al_2O_3 support. The peak labels and peak temperatures at initial saturation coverage are listed in Table 1.

To characterize the desorption process more accurately, the desorption peaks were recorded at lower initial surface coverages. Figure 2 shows a series of H_2/N_2H_4 for different initial exposures to N_2H_4. At low coverages only the $H_2(\beta)$ peak was occupied, and with additional hydrazine exposure, the $H_2(\alpha)$ peak became filled. Also, it was noted that with decreasing N_2H_4 exposure, the total mass of NH_3 adsorbate diminished and the NH_3 desorption shifted to higher temperature values. A series of N_2/N_2H_4 desorption studies at different initial coverages demonstrated that lowering of the surface coverages caused the β peak to decrease and the α peak to increase (Figure 3).

To provide additional detail on the desorption kinetics involved in nitrogen formation, a series of TPD experiments were carried out

after N_2H_4 exposure of the catalyst at 275°C. By using such a high initial surface temperature we were able to eliminate the $H_2(\alpha)/N_2H_4$, the $NH_3(\alpha_1)/N_2H_4$, and most of the $NH_3(\alpha_2)/N_2H_4$. The resultant N_2/N_2H_4 (275) TPD spectra, shown in Figure 4, indicated that the $N_2(\beta_2)/N_2H_4$ peak temperature did not change with initial surface coverage, i.e., the N_2 was formed by a first-order process. Although the $H_2(\beta)/N_2H_4(275)$ peak exhibited a higher peak temperature than the $N_2/N_2H_4(275)$ peak and a much larger temperature tail, the total mass ratio of $H_2(\beta):N_2(\beta_2)$ was (3.2 ± 0.2):1 after exposure of the Ir-catalyst to saturation N_2H_4 coverage at 275°C.

By varying the heating rate (0.25 Ks^{-1} ≤ β ≤ 3.6 Ks^{-1}), we determined the activation energy for formation of the well-defined $N_2(\beta_2)/N_2H_4$ at corstant initial saturation surface coverage. As the heating rate β increased, the desorption curves shifted to higher temperatures and increased in amplitude, but the total mass of adsorbate remained the same. From the changes in T_p (peak temperature) and N_p (peak amplitude) with β, the activation energy, E, could be determined without knowledge of the preexponential factor.[5,6] Figure 5 shows the resultant plots of $\ln(\beta/T_p^2)$ versus $1/T_p$ and $\ln N_p$ versus $1/T_p$. From the slope of the lines analyzed by least-squares fit of the data, one obtained activation energies of 27.4 kcal/mol (Figure 5a) and 26.2 kcal/mol (Figure 5b). From the intercept of the curve in Figure 5a, the preexponential factor can be determined on the basis of a first-order reaction, as indicated by the constancy of the peak desorption temperature with coverage. Using the average value of E [$N_2(\beta_2)/N_2H_4$] = 26.8 kcal/mol, we calculated a preexponential factor of 3×10^7 s^{-1}.

Desorption Studies with Used Catalyst (Shell-405)

TPD spectra were obtained for catalyst B, a sample that had been exposed to N_2H_4 in a rocket thruster (cf. Section B). The

desorption peak temperatures and the relative surface population of the different adspecies (Figure 6) showed close similarity to those obtained for catalyst A (Figure 1). However, the total mass of adsorbate, as determined from the integrated areas under the TPD curves, demonstrated marked differences (Table 2). Also, the surface area of these catalysts, measured after the TPD experiments, was found to have decreased appreciably (Table 2).

3. Effect of Hydrogen Adatoms on Hydrazine Decomposition

Hydrogen was coadsorbed with hydrazine on fresh Catalyst A to obtain a better understanding of the decomposition mechanism. A steady flow of H_2 in He was maintained over the surface, while liquid hydrazine was injected through the septum. After a given exposure to reactant, TPD spectra were obtained both in the presence and absence of H_2 in the carrier stream.

For NH_3 N_2H_4, N_2/N_2H_4, and H_2/N_2H_4, the differences in desorption characteristics with and without H_2 coadsorption were found to be within the experimental error ($\pm$ 10%). The products formed from N_2H_4 decomposition also remained unaffected by hydrogen.

4. Steady-State Flow Experiments

To examine the product distribution resulting from the Ir-catalyzed decomposition of N_2H_4 over a range of temperatures, 3 μl samples of N_2H_4 were injected into the reactor containing catalysts A or B, and the reaction products were monitored by mass spectrometry. The mass of injected N_2H_4 was large relative to the amount remaining adsorbed on the surface. Steady-state activity was verified by product analysis for repeated injections of 3 μl N_2H_4 at a given temperature, which ranged from 25 C to 800 C. Product gases were injected for

calibrations at frequent intervals, so that absolute quantities of products could be determined. Figure 7 shows the amounts of N_2, H_2, and NH_3 produced per mole of N_2H_4 in the presence of catalyst A. Below 300°C hydrazine decomposes almost exclusively to form N_2 and NH_3 according to the stoichiometry:

$$3\ N_2H_4 \rightarrow N_2 + 4\ NH_3 \qquad (1)$$

and above 600°C to form N_2 and H_2 with the stoichiometry:

$$N_2H_4 \rightarrow N_2 + 2H_2 \qquad (2)$$

At intermediate temperatures both reactions contribute to the product distributions.

Similar experiments were performed with NH_3 as the reactant by injecting 1000 µl of gaseous NH_3 and observing the decomposition products as a function of catalyst temperature. Figure 8 shows the amount of N_2 formed and the amount of undecomposed NH_3 per mole of injected NH_3. Below 300°C we observed little NH_3 decomposition on catalyst A; however, above 600°C all of the NH_3 decomposed to N_2 and H_2 with a satisfactory mass balance.

A series of runs were carried out in which catalyst A was continuously exposed to N_2H_4 for prolonged time periods at temperatures from 25°C to 435°C. A syringe pump provided continuous feed rates of 2 to 10 µl liquid N_2H_4 per minute. The total cumulative exposure was equivalent to 1.1 moles N_2H_4 per gram of catalyst. Also, the catalyst was given many heating cycles to 750°C after N_2H_4 exposure. For all flow rates used complete reaction occurred at and above room temperature under our experimental conditions. While TPD studies did not reveal any differences in desorption characteristics of the catalyst after prolonged exposure to N_2H_4, the iridium surface area of catalyst A had

decreased from 51 m^2/g Ir to 44.7 m^2/g Ir. By way of comparison, catalyst B, which was used in a rocket thruster and had been exposed to 1097 moles N_2H_4 per gram catalyst, had a surface area of 27.5 m^2/g Ir.

DISCUSSION

In elucidating the mechanism of the Ir-catalyzed decomposition of hydrazine, it is important to examine the conditions that affect rupture of the N-N bond, i.e., dissociative versus non-dissociative adsorption. Thus, to determine whether the TPD products following hydrazine exposure are reaction or desorption limited, a study was carried out of the TPD characteristics of some of the products observed.

In the case of ammonia, the TPD spectra of N_2, H_2, and NH_3 following ammonia adsorption on the Ir/Al_2O_3 catalyst at room temperature are shown in Figure 9. The NH_3/NH_3 desorption exhibited a major peak at 140 °C and another one near 335 °C. The H_2/NH_3 and N_2/NH_3 were found to desorb in a 3:1 ratio at nearly the same peak temperature (Table 1). Therefore, one may conclude that they were formed from the same adsorbed species, an ammonia molecule. A comparison of the data in Figures 1 and 9 indicates strong similarities between the sorption characteristics of NH_3 and N_2H_4 on Ir/Al_2O_3. The NH_3/NH_3 and NH_3/N_2H_4 TPD peaks occur at the same temperature, and the surface coverages with each of these species are nearly the same (Table 2). Also, the $N_2(\beta)/NH_3$ and $H_2(\beta)/N_2H_4$ peaks are similar, expecially in comparison with H_2/N_2H_4 at low hydrazine coverages, where the $H_2(\alpha)/N_2H_4$ peak is absent (Figure 2). The TPD in Figure 2 indicates that the $H_2(\alpha)/N_2H_4$ peak corresponds to $H_2(\alpha)/H_2$. Finally, the N_2/N_2H_4 and N_2/NH_3 peaks exhibit similarities, although the N_2/N_2H_4 peak is smaller than the N_2/NH_3 peak at high N_2H_4 exposure (Figure 3). The strongly bound $N_2(\beta_2)$, with a peak desorption temperature of 390 °C,

is essentially the same for N_2/NH_3 and N_2/N_2H_4. But following NH_3 adsorption an additional peak $N_2(\beta_1)$ is observed, which was detected only at low hydrazine coverages. The origin of $N_2(\beta_1)$ is uncertain. It may be due to the existence of an oxygen adsorbate on the Ir-surface, which is removed at room temperature by exposure to hydrazine but not reduced by NH_3. As a matter of fact, the two distinct N_2/N_2H_4 spectra shown in Figure 10 for saturation N_2H_4 coverage at room temperature indicate the effect of adsorbed oxygen on catalyst A. Curve (a) was obtained after the first exposure of the catalyst to N_2H_4. A similar curve was also obtained following N_2H_4 exposure to catalyst A after brief oxygen contact. Curve (b) represents the reproducible spectra obtained for N_2/N_2H_4 on the reduced catalyst. It is identical to the spectra in Figure 1. Curve (a) corresponds to a total surface coverage of 4.9×10^{19} N_2 molecules/g catalyst, while curve (b) to 1.5×10^{19} N_2 molecules/g catalyst. These results indicate that in the presence of oxygen adatoms the nitrogen coverage is increased and its binding energy reduced.

TPD spectra were also obtained for H_2O/H_2O and H_2O/H_2. Comparison with H_2O/N_2H_4 indicates the H_2O/N_2H_4 was due to hydrogen formed during the hydrazine decomposition. Thus, the H_2O/N_2H_4 did not result from the presence of water in the hydrazine, but more likely from adsorbed hydrogen atoms, which reacted with alumina OH-groups or reduced the surface-oxidized iridium with water as a product.[2]

Using the slope and intercept obtained from the heating rate variation for $N_2(\beta_2)/N_2H_4$, we found that the adsorbed intermediate that yielded N_2 and H_2 products decomposed with a first-order rate constant equal to $3 \times 10^7 \exp(26,800/RT)\ s^{-1}$. A first-order rate expression with this rate constant was integrated numerically for a 2 Ks^{-1} heating rate as a function of temperature to determine the expected desorption curve.

The dashed curve in Figure 10 corresponds to that integration, and the agreement with the experimentally observed curve is quite good.

By comparison with the NH_3 experiments we conclude that the H_2- and N_2-peaks formed during N_2H_4 decomposition at room temperature originate from an adsorbed ammonia intermediate, as suggested by the H_2:N_2 ratio and the similarity of the H_2/N_2H_4 and N_2/N_2H_4 peaks to H_2/NH_3 and N_2/NH_3. The similarity between N_2/N_2H_4 and N_2/NH_3 strongly suggests rupture of the N-N bond on adsorption of N_2H_4 and formation of an adsorbed intermediate. The decomposition of this intermediate leads to the formation of N_2 and H_2 with a kinetic order of unity. Studies with N-15-labelled hydrazine have indicated the absence of isotope mixing in the N_2 formed from N_2H_4 decomposition on Fe-on-MgO catalyst at temperatures from 26 to 350°C.[7] Isotope mixing did not occur for labelled N_2H_4 decomposition on quartz at 270-325°C,[8] nor for liquid phase decomposition on Shell-405,[9] nor on Rh[10] at room temperature. All these isotopic studies were carried out at relatively low temperatures where N_2 and NH_3 were the predominant products and little NH_3 decomposition took place. Similarly, in our studies with Shell-405 at temperatures below 325°C, the amount of NH_3 decomposition, or the amount of H_2 production from N_2H_4, was very small. It appears that in the temperature regime in which Reaction (1) predominates, the adosrption is non-dissociative. However, at higher temperatures where N_2 and H_2 become the predominant products, rupture of the N-N bond prevails. The N_2/N_2H_4 desorption from Shell-405 catalyst requires sufficiently high temperatures to cause dissociation of the surface-adsorbed intermediate. We must conclude that $N_2(P_2)/N_2H_4$ is formed by an entirely different pathway from the N_2 produced in Reaction (1), as discussed in further detail in Reference 1.

The reaction mechanism on the Al_2O_3-supported Ir-catalyst may be similar to that proposed for the polycrystalline iridium foil. But some

significant differences are noted. Below 200°C, it was proposed that adsorption on the foil occurs according to Equation (3)

$$N_2H_4 \rightarrow H - \underset{*}{N} - \underset{*}{N} - H + 2H^* \qquad (3)$$

where the asterisk indicates adsorbed species. A gas phase N_2H_4 molecule reacted with $N_2H_2^*$ to form NH_3 and N_2.

$$N_2H_2^* + N_2H_4 \rightarrow N_2 + 2NH_3 \qquad (4)$$

This reaction resulted in the formation of N_2 without rupture of the N-N bond in N_2H_4. Also, this mechanism is consistent with the observation that hydrazine decomposition occurs on a surface saturated with adspecies. Indeed, following long exposure to N_2H_4 at room temperature the CO, O_2 titration technique indicated no bare iridium metal. Heating to 300°C in H_2 and then in He removed the adsorbed surface species, and a CO, O_2 titration yielded the same iridium surface area observed before N_2H_4 exposure.

If, as on the foil, Reaction (3) was the pathway to hydrazine decomposition, the subsequent reactions were different for the supported catalyst during steady-state decomposition. On the foil, adsorbed hydrogen atoms recombined and desorbed; on the supported catalyst, almost no gaseous H_2 was formed below 200°C (see Figure 7). Though no H_2 was formed below 200°C, adsorbed hydrogen was present on the surface, as indicated by the TPD spectra (Figure 1). Thus, for the stoichiometry in Equation (1) to be satisfied, the reaction

$$N_2H_4 \rightarrow 2NH_2^* \qquad (5)$$

$$NH_2^* + H^* \rightarrow NH_3^* \qquad (6)$$

may be occurring. The results suggest that on the small Ir-crystallites

of Shell-405 below 200°C, Reaction (6) is more rapid than hydrogen atom recombination. This may be because the hydrogen is more strongly bound on the supported catalysts than on the foil. The NH_3 formed (Equation 6) desorbs as the surface becomes saturated so that the overall result of Equations (3)-(6) was Reaction (1). Ammonia adsorbed on the surface gave similar desorption characteristics. Since H^* is absent in the latter case, the rate-limiting step in NH_3 formation from hydrazine must be the desorption process rather than Equation (6).

Prolonged exposure of the catalyst to hydrazine (i.e., equivalent to many monolayers) and subsequent TPD did not yield the product species in the same ratio observed during steady-state decomposition. At room temperature, N_2 and NH_3 were the only steady-state reaction products, but during TPD a substantial H_2/N_2H_4 peak was observed in addition to N_2 and NH_3. Apparently, NH_3 and some H_2 formed during steady-state decomposition remain on the Ir surface or on the Al_2O_3 support with a binding energy sufficiently large to prevent desorption at room temperature. Since Ir does not chemisorb nitrogen from the molecular state[2,11,12] the N_2 observed does not arise from readsorption of the nitrogen molecule on the catalyst surface.

In comparing the TPD spectra for catalysts A and B, we observed in the latter case lower surface densities of all the adspecies (H_2, N_2, NH_3), but no change in their respective binding states (Table 2). This decrease in surface population correlates with a diminution in iridium surface area. Assuming that all the desorbed products originate from metal sites, we can calculate a surface coverage per cm^2 of iridium. These values are listed in Table 3 for the fresh and used catalysts. As yet it has not been ascertained whether the change in active surface area is due to sintering of the dispersed iridium crystallites or surface poisoning by species so strongly bound that they do not desorb during TPD. Brooks[13] has carried out adsorption experiments on samples of

Shell-405 catalyst and obtained similar results. In particular, on a used catalyst he observed a decrease in mass of H_2 and O_2 adsorbed. He attributed these changes to increases in the iridium metal crystallite size. The changes in Ir-surface area derived from H_2-chemisorption studies[13] correspond to those obtained in our study with the CO,O_2 titration technique.

In addition, our results with Shell-405 catalyst are qualitatively similar to the data reported by Contour and Pannetier[2] on an Ir/Al_2O_3 catalyst prepared by them. However, their N_2/N_2H_4 desorption results exhibit lower peak temperature (around 200°C) and are interpreted in terms of second-order kinetics with an activation energy of 14 kcal/mole. This discrepancy with our data for $N_2(P_2)/N_2H_4$ may be indicative of differences in catalyst preparation and catalyst support.

Recent flash desorption experiments with hydrazine adsorbed on a Pd wire[14] exhibit interesting differences from the properties of Ir-catalyst (Shell-405). In the case of Pd the N_2/N_2H_4 and H_2/N_2H_4 products desorb at the same temperature (100°C), but experimental difficulties prevented observation of NH_3 desorption. Ertl and Tornau[14] postulate that the rate limiting step is successive hydrogen abstraction to form N_2 and H_2 from adsorbed N_2H_4 without rupture of the N-N bond. Experiments on steady-state decomposition catalyzed by Pd[14] demonstrated complete reaction at 180°C. However, similar to the iridium foil, there was no temperature regime in which NH_3 and N_2 were the only reaction products as observed in our study with supported Ir-catalyst. A comparison of N_2H_4 decomposition rates and the surface binding states associated with N_2/N_2H_4 on Ir and Pd indicates that a strong adsorbate surface bond is required for efficient N_2H_4 decomposition. Possibly, it is the lifetime of N_2H_2-surface intermediate (Equation 3) that governs the catalytic activity for hydrazine decomposition.

The TPD spectra from a polycrystalline iridium foil following N_2H_4 and NH_3 exposure[1] exhibit qualitative agreement with the spectra from Shell-405. One difference of special interest is the data for N_2/N_2H_4 for which three peak desorption temperatures were recorded for the Ir-foil (~150°C, ~380°C, and ~645°C). The observation that for the Ir-foil the N_2/N_2H_4 peak temperature of 380°C is identical to that for N_2/NH_3 and H_2/NH_3, suggests strongly that this binding state corresponds to $N_2(\beta_2)/N_2H_4$ on Shell-405 catalyst. The most strongly bound state corresponding to a peak desorption temperature at 645°C on the Ir-foil was not observed on the supported Ir-catalyst. However, a strongly bound nitrogen species that could not be flashed off at temperatures as high as 975°C was detected by Auger spectroscopy following exposure of Shell-405 to hydrazine. It must be concluded that surface binding energies are affected by crystal orientation and surface defects, as a result of which quantitative correlation between the properties for polycrystalline Ir and supported Ir-crystallites is not to be expected. On the other hand the results for steady-state decomposition of N_2H_4 on the supported Ir-catalyst (Figure 7 and 8) and the polycrystalline foil, exhibit greater similarities. Although the degree of N_2H_4 conversion was smaller on the Ir-foil because of differences in metal surface area, the results from low-pressure studies on the polycrystalline foil are consistent with those from the supported catalyst at atmospheric pressure.

The transition in product distribution from Reaction (1) (with NH_3 and N_2 as products) to Reaction (2) (with H_2 and N_2 as products) is interpretable in terms of the TPD data of the adsorbed surface species resulting from hydrazine decomposition. The rate constant k equal to $3 \times 10^7 \exp(-26{,}800/RT)\ s^{-1}$ for $N_2(\beta_2)$ formation indicates that at 330°C, where Reaction (1) occurs exclusively, the reaction time constant (1/k) is 200 s, so that NH_3 desorption would be favored over its decomposition

to N_2 and H_2. On the other hand, at 630°C, where Reaction (2) occurs exclusively, the reaction time constant is less than 0.1 s, so that N_2 and H_2 formation would be favored over NH_3 desorption, especially since the activation energy for NH_3 desorption[2] is small (~10 kcal/mol). These results indicate the usefulness of detailed TPD spectra for determination of reaction selectivity.

CONCLUSIONS

Exposure of the alumina-supported Ir-catalyst (Shell-405) to hydrazine leads to the formation of surface-adsorbed intermediates that yield H_2, N_2, and NH_3 during temperature programmed desorption. Their binding states are of sufficient magnitude to require elevated temperatures for desorption. The $N_2(\beta_2)$-state, the most strongly bound state observed for Ir/Al_2O_3, exhibits a peak desorption temperature of 380°C. Steady-state catalytic decomposition yields NH_3 and N_2 at temperatures below 300°C, and N_2 and H_2 at temperatures above 500°C, a region in which NH_3 begins to dissociate. Qualitatively, the dispersed Ir-crystallites exhibited similar surface properties to those observed for polycrystalline iridium, and crystal structure-sensitive binding states may account for the differences observed.

A comparison of the surface properties of fresh and used Ir/Al_2O_3 catalyst has demonstrated a loss in active metal surface area caused by prolonged exposure of the catalyst to hydrazine in a laboratory reactor or in a monopropellant thruster. This change is accompanied by a decrease in the number density of surface sites available for adsorption during N_2H_4 exposure, without the disappearance of a specific binding state. It has not been ascertained whether this surface area decrease is the result of thermal sintering of the Ir-crystallites or the buildup of an irreversibly adsorbed surface species that originates during hydrazine decomposition.

REFERENCES

1. B. J. Wood and H. Wise, J. Catalysis, in press.

2. J. P. Contour and G. Pannetier, J. Catalysis 24, 434 (1972).

3. P. Wentrcek, K. Kimoto, and H. Wise, J. Catalysis 33, 279 (1973).

4. P. Wentrcek and H. Wise (in preparation).

5. P. A. Redhead, Vacuum 12, 203 (1962).

6. J. L. Falconer and R. J. Madix, Surface Sci. 43, 393 (1975).

7. J. Block and G. Schulz-Ekloff, J. Catalysis 30, 327 (1973).

8. A. Kant and W. J. McMahon, J. Inorg.-Nucl. Chem. 15, 305 (1960).

9. C. F. Sayer, Rocket Propulsion Establishment Technical Report No. 69/10, December 1969.

10. K. M. Davis and C. F. Sayer, Trans. Far. Soc. 68, 1894 (1972).

11. V. J. Mineault and R. S. Hansen, J. Phys. Chem. 70, 3000 (1966).

12. B. E. Nieuwenhuys, D. Th. Meijer, and W.M.H. Sachtler, Surface Sci. 40, 125 (1973).

13. C. S. Brooks, J. Colloid and Interface Science 34, 419 (1970).

14. G. Ertl and J. Tornau, Z. Physik. Chem. Neue Folge 93, 109 (1974).

Table 1

TEMPERATURE PROGRAMMED DESORPTION PEAKS FOR
Ir/Al_2O_3 (SHELL-405) CATALYST

Product \ Adsorbate	Temperature (°C)			
	N_2H_4	NH_3	H_2	H_2O
N_2	390 (β_1) ~315 (β_1^1)	390 (β_2) 310 (β_2^2)	-	-
H_2	400 (β) 175 (α)	400 (β)	135 (α)	-
NH_3	335 (α_2) 140 (α_1^2)	335 (α_2) 140 (α_1^2)	-	-
H_2O	Broad peak at 800°C	-	Broad peak at 800	320 (α_2) 107 (α_1^2)
N_2*	355 (β) 180 (α_2) 100 (α_1^2)			

*On catalyst pre-exposed to oxygen.

Table 2

SURFACE COVERAGES FOR Ir/Al_2O_3 CATALYST (SHELL-405) (RRC)

Product/Adsorbate	Surface Adsorbate ($\times 10^{-19}$ molecules/g Catalyst)		Relative Change (%)
	Catalyst A*	Catalyst B*	
H_2/H_2	7.2	4.2	42
H_2/NH_3	-	3.2	-
H_2/N_2H_4	8.2	5.4	34
H_2/N_2H_4(275)	4.1	3.3	20
N_2/N_2	zero	zero	-
N_2/NH_3	2.1	1.2	43
N_2/N_2H_4	1.5	0.9	40
N_2/N_2H_4(275)	1.3	-	-
NH_3/NH_3	9.7	6.1	40
NH_3/N_2H_4	9.7	6.5	35
H_2O/H_2O	21.2	-	-
Iridium Surface Area (m^2/g Ir)	44.9**	27.5	39

*Samples from Rocket Research Corporation, Redmond, Wash.

**This catalyst had been exposed to a series of TPD experiments as a result of which its surface area was somewhat lower than the original value (cf. text).

Table 3

SPECIFIC SURFACE COVERAGES FOR Ir/Al_2O_3 (SHELL-405)*

Product/Adsorbate	Surface Population ($\times 10^{-14}$ molecules/cm^2 Ir)	
	Catalyst A**	Catalyst B**
H_2/H_2	5.1	4.6
H_2/N_2H_4	5.7	6.2
H_2/N_2H_4(275)	2.9	3.8
N_2/NH_3	1.5	1.4
N_2/N_2H_4	1.0	1.0
NH_3/NH_3	6.9	6.9
NH_3/N_2H_4	6.8	7.4

*Coverages were calculated under the assumption that all the desorption was from the iridium surface and none from the alumina.

**Samples from Rocket Research Corp., Redmond, Washington.

List of Illustrations

Figure

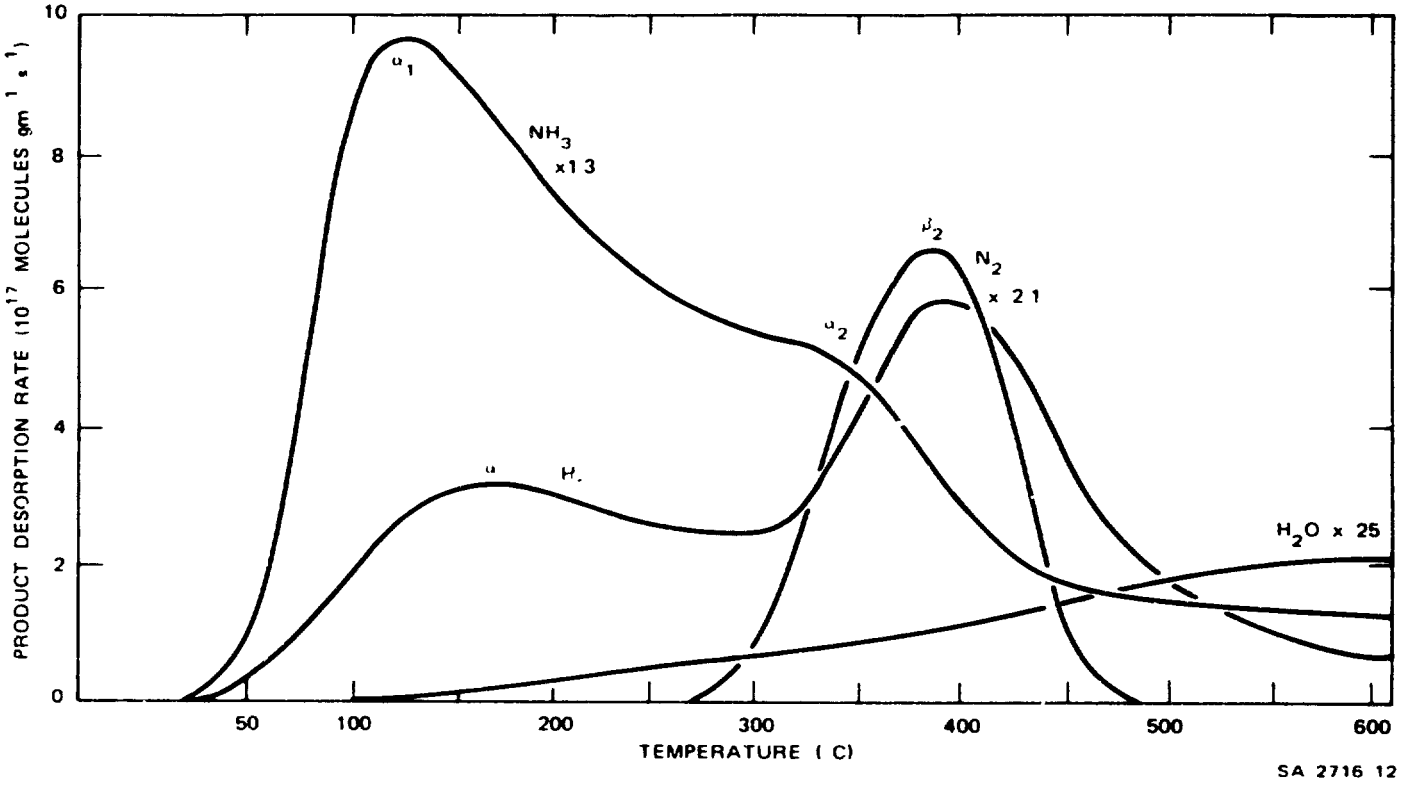

FIGURE 1 NH_3, H_2, N_2, AND H_2O TPD PEAKS FOR N_2H_4 ADSORPTION (SATURATION COVERAGE) ON FRESH SHELL 405 CATALYST

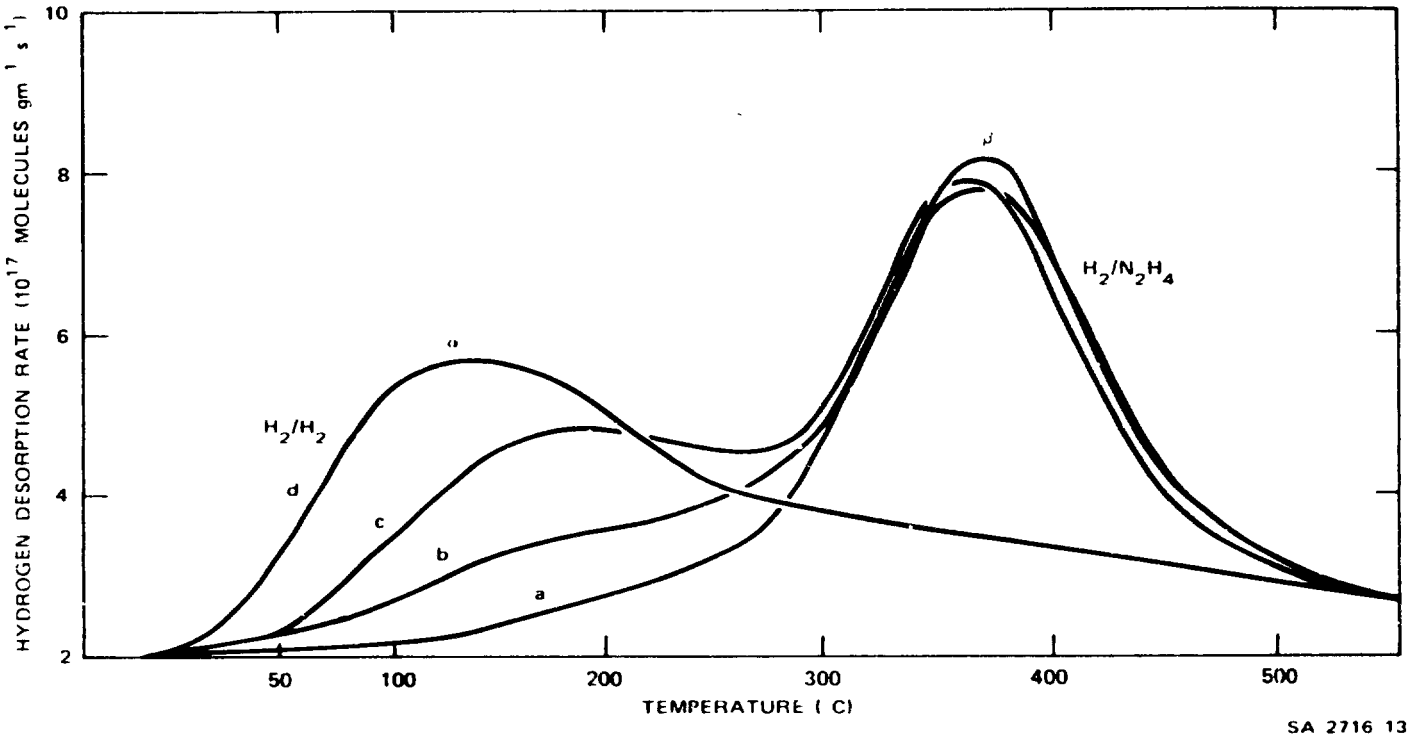

FIGURE 2 H_2/N_2H_4 TPD SPECTRA

Exposures in $\mu\ell$ N_2H_4. (a) 1, (b) 2, (c) 5, (d) H_2/H_2 flash desorption for saturation exposure.

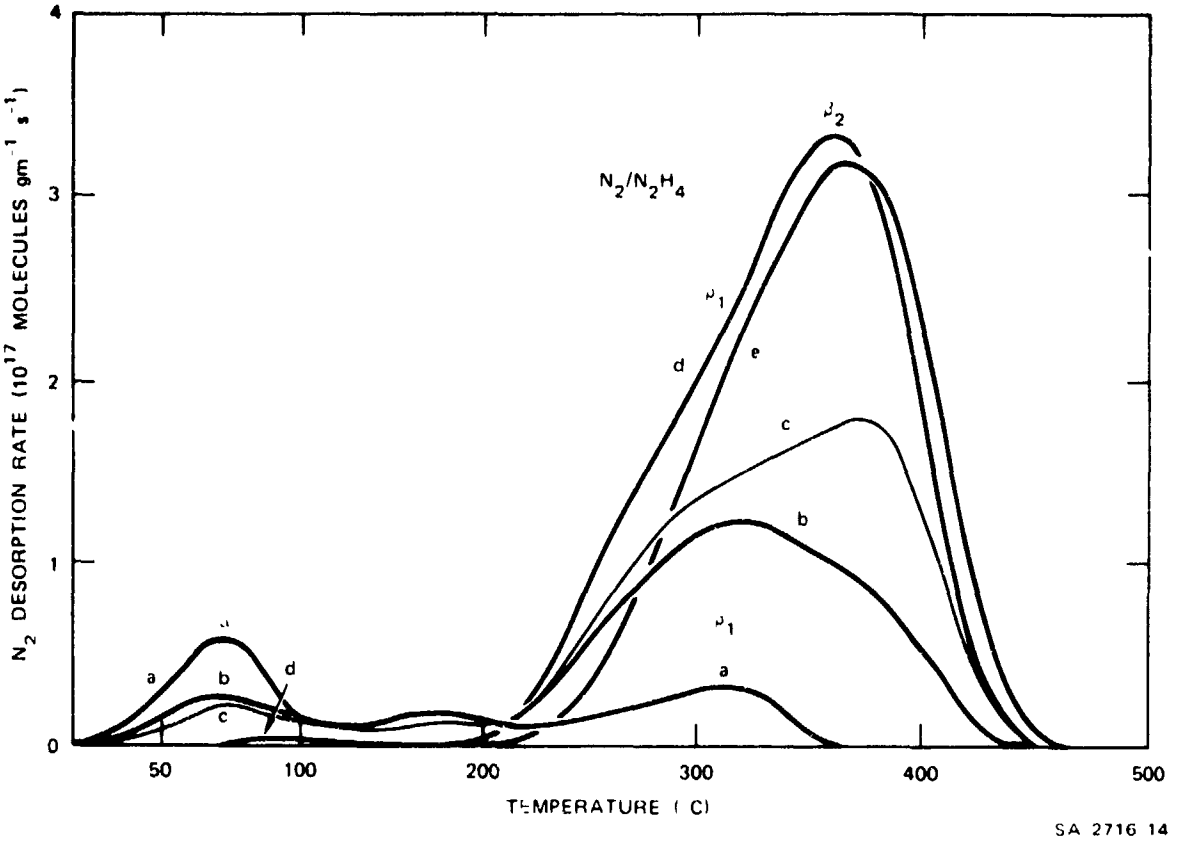

FIGURE 3 N_2/N_2H_4 TPD SPECTRA

Exposures in $\mu\ell$ N_2H_4 (a) 0.02, (b) 0.05, (c) 0.1, (d) 0.3, (e) 1.0

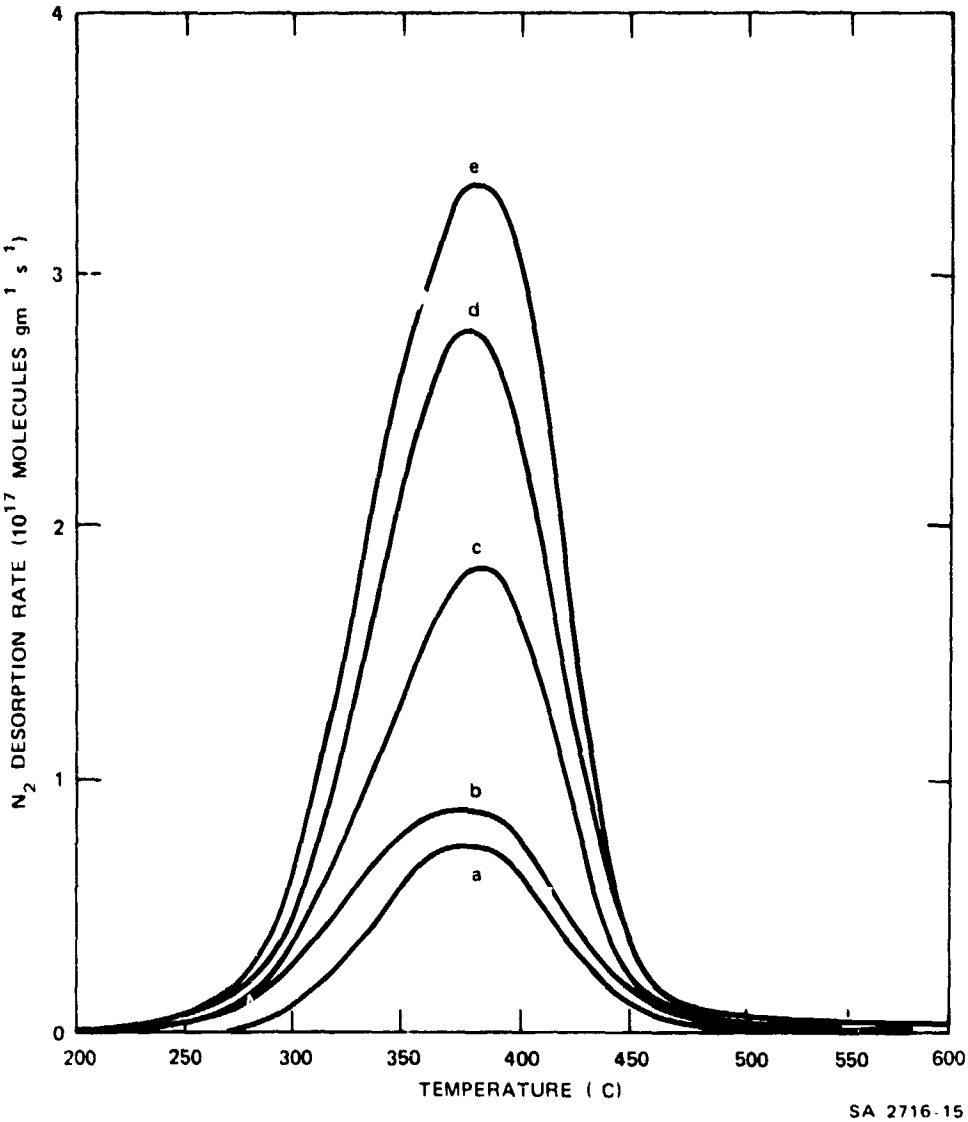

FIGURE 4 N_2/N_2H_4 (275) TPD SPECTRA

Exposures in μV N_2H_4 (a) 0.02, (b) 0.035, (c) 0.05, (d) 0.1, (e) 5.0

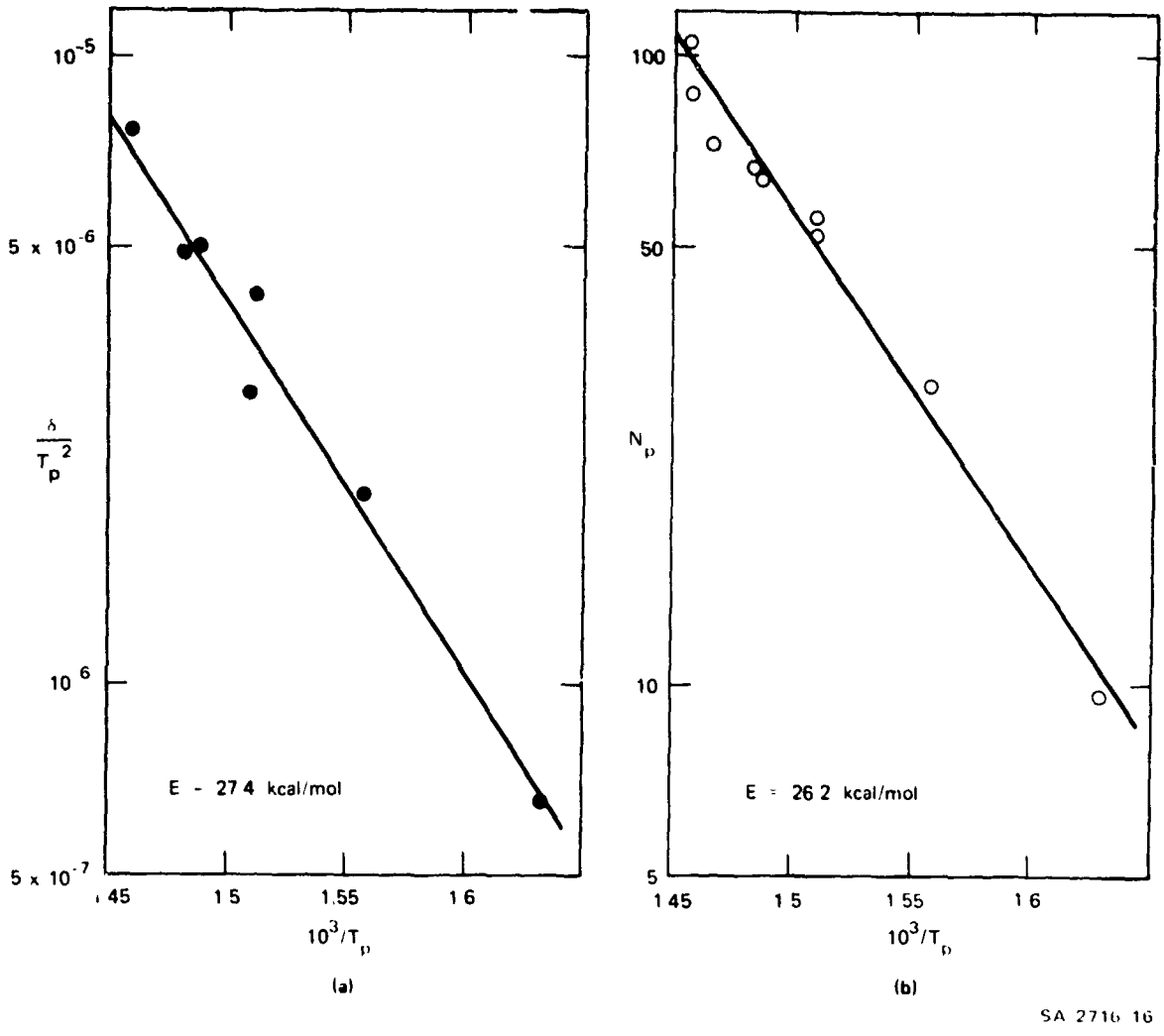

FIGURE 5 ACTIVATION ENERGY DETERMINATION FROM HEATING RATE VARIATION
(a) $\ln (\delta T_p^2)$ versus $1/T_p$ for $N_2(\beta_2)/N_2H_4$. (b) $\ln N_p$ versus $1/T_p$ for $N_2(\beta_2)/N_2H_4$

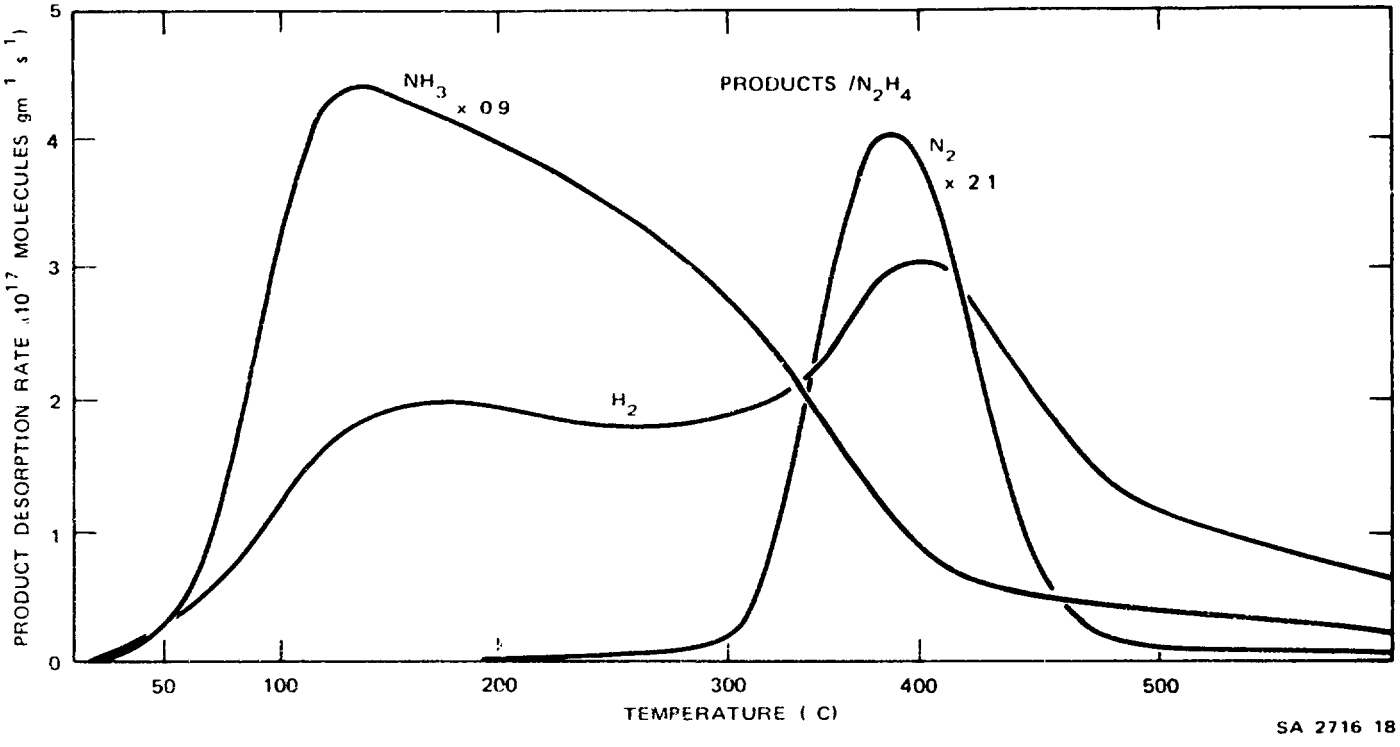

FIGURE 6 NH_3, N_2, AND H_2 TPD PEAKS FOR N_2H_4 ADSORPTION (SATURATION COVERAGE) ON USED SHELL 405 CATALYST

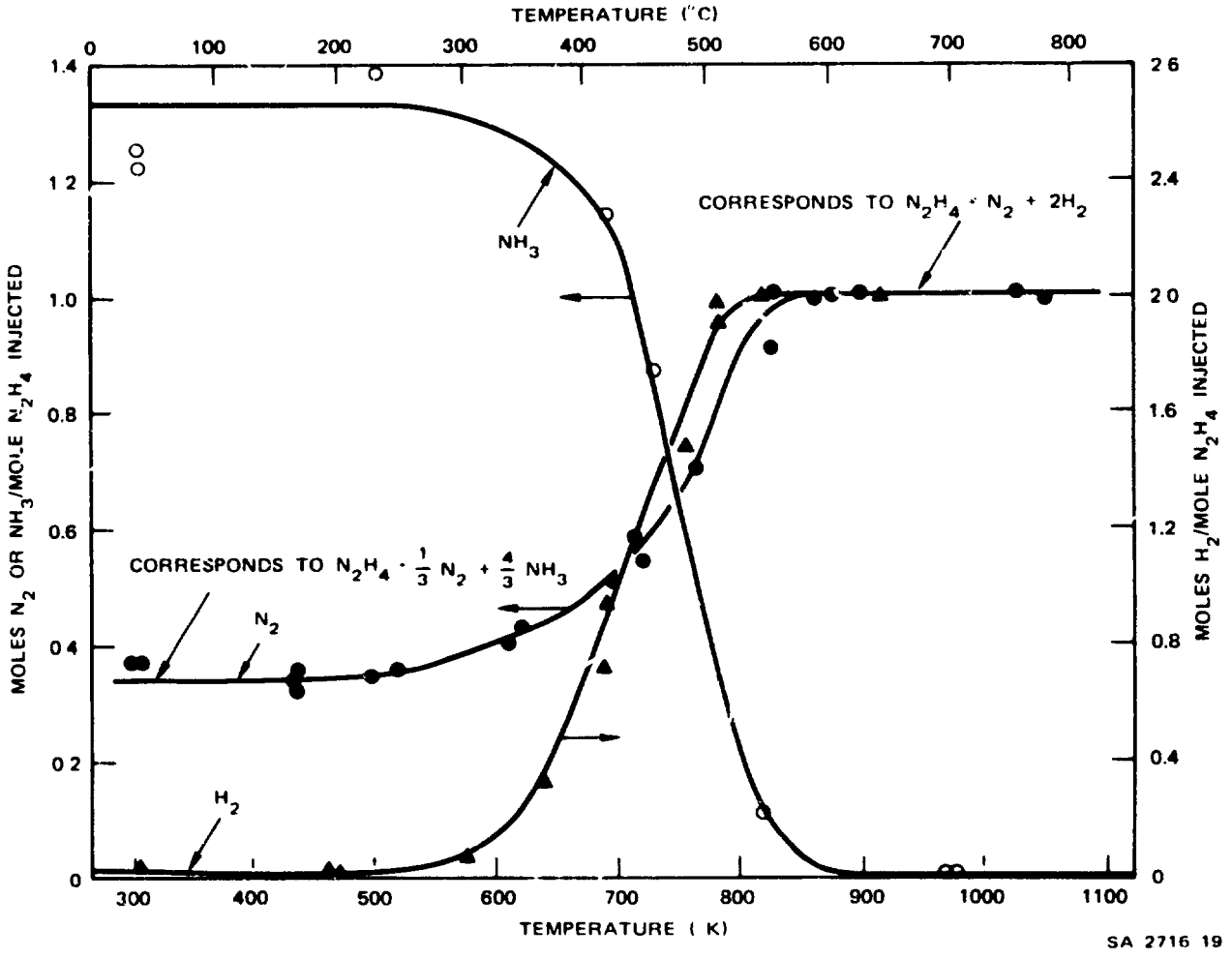

FIGURE 7 PRODUCTS OF N_2H_4 DECOMPOSITION CATALYZED BY SHELL 405 CATALYST AT DIFFERENT TEMPERATURES (DATA COLLECTED DURING RESPONSE OF CATALYST TO A SERIES OF 3 μl ALIQUOTS OF LIQUID N_2H_4)

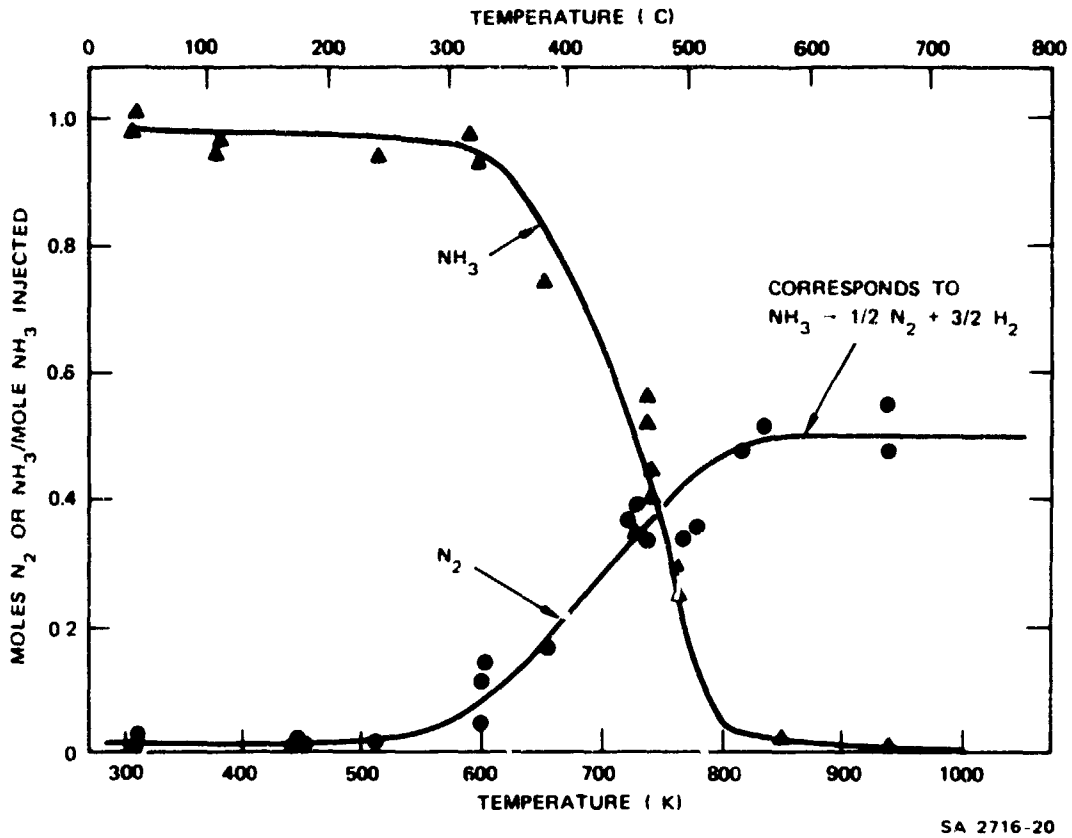

FIGURE 8 PRODUCTS OF NH_3 DECOMPOSITION CATALYZED BY SHELL 405 CATALYST AT DIFFERENT TEMPERATURES (DATA COLLECTED DURING RESPONSE OF CATALYST TO A SERIES OF 1000 μl ALIQUOTS OF GASEOUS NH_3)

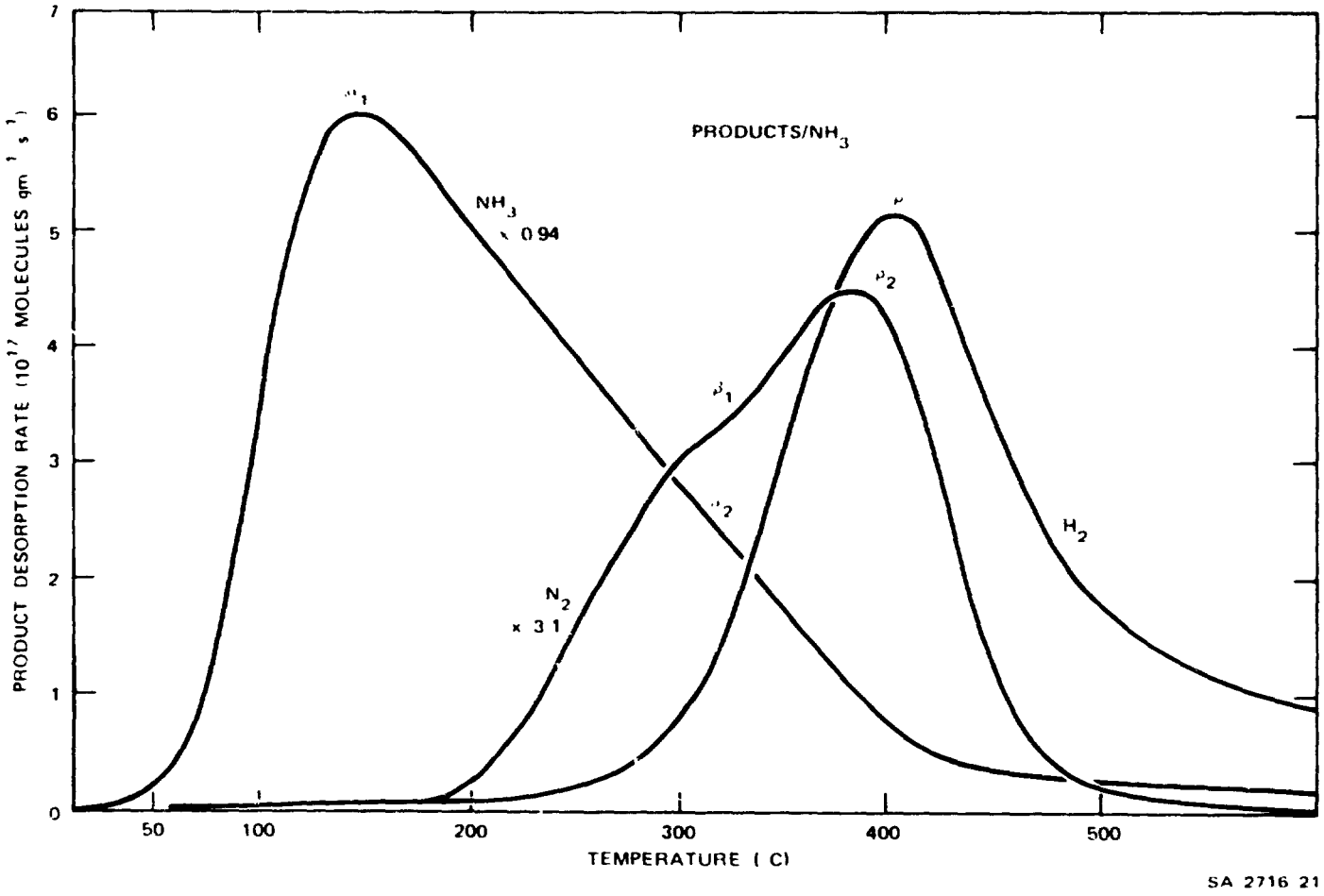

FIGURE 9 NH_3, H_2, AND N_2 TPD PEAKS FOR NH_3 ADSORPTION (SATURATION COVERAGE) ON FRESH SHELL 405 CATALYST

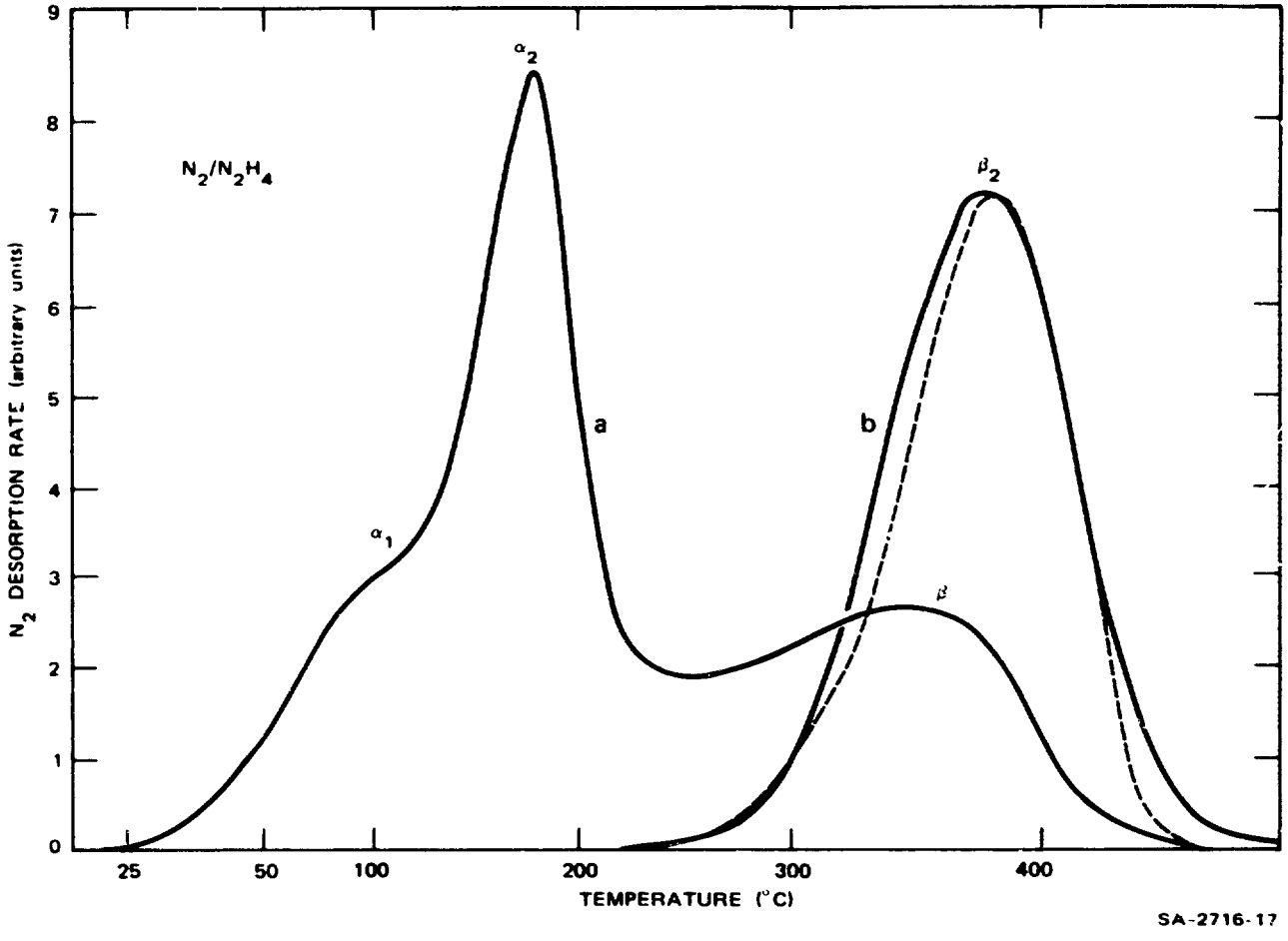

FIGURE 10 N_2/N_2H_4 TPD PEAKS FOR SATURATION N_2H_4 COVERAGE ON (a) OXIDIZED CATALYST (b) REDUCED CATALYST

Dashed line is theoretical first-order desorption curve for rate constant of $3 \times 10^7 \exp(26{,}800/RT)s^{-1}$.